Dear Professor Joos, dear reviewer,

Thank you for your thorough feedback on our revised manuscript from the 5th of June, 2018. We very much appreciate the time and effort you have spent on our manuscript. We addressed each comment and concern, and hereby present our newly revised version. Please, find details about the changes made relative to the last version of the manuscript in the responses below and in the marked-up manuscript.

The author's response is presented as follows:

(1) **Referee report**: comments from the reviewer report with author's response to each comment and summary of author's changes in the manuscript,
(2) **Editor comments**: comments from the editor with author's response to each comment and summary of author's changes in the manuscript,
(3) **Marked-up manuscript**: Author's changes tracked in the new manuscript

Yours sincerely, Anne Morée and co-authors

Referee report

Comment 1.1) Appreciation of the replies to reviewers

The authors have all in all well responded to the referees' comments, with two exceptions.
1. The questions raised by Anonymous Referee #2 about the weathering fluxes have only partly been addressed. Except for the average δ 13C signature of the DIC input from weathering, there is still no information regarding the quantitative constraints upon which the adopted weathering fluxes have been chosen (it would also be good to know their values).
2. In the response to Comment 2.2.3, I read that "In an open system, the sediment loss of nutrients and carbon over time will empty the whole ocean of nutrients, which would not give very meaningful results." This cannot be correct. As explained earlier on, PO3− 4 is replenished by the (constant) weathering input. Upon perturbation, the model system adjusts its carbonate, organic matter and opal production and burial fluxes to evolve towards a new steady state where burial fluxes again match the input fluxes. The ocean will not run empty, as the production decreases with decreasing nutrient concentrations thus reducing the burial rates.

Author response to Comment 1.1)

Thank you for providing us with a clear review of our latest manuscript. The two exceptions mentioned here in comment 1.1 are addressed by:
1. Extending the Methods (Sect 2) text on the weathering fluxes with stoichiometric ratios, absolute fluxes and a comparison to observational estimates (see also our reply to comment 2.1.1)
2. Our formulation of our reply was indeed not detailed enough and therefore misleading/incorrect. As this mistake is not made in the manuscript, no further large changes have been made there. We did add the word 'transient' (POC sinking rate experiments) to clarify that the imbalance between burial and weathering is temporary. What we meant to write in our previous response is that there will be a decrease of nutrients until a new equilibrium is established based on the weathering fluxes, such that input and burial are in mass balance. As this equilibration takes hundreds of thousands of years (Roth et al., 2014) for $\delta^{13}C$, we decided to present transient results for the POC experiments, as reasoned for in our previous reply.

Author's changes in the manuscript in response to Comment 1.1)

- The methods text on weathering is extended to include the missing information on that subject.
- The word 'transient' has been added to further stress that the weathering-burial imbalance of the POC experiments is temporary

Comment 1.2) Appreciation of the revised manuscript

The authors have rewritten their manuscript to a large extent. The language has gained in precision and the presentation and discussion in depth. The literature review is adequate now and the study is much better brought into context with previous studies. The model description has been improved. The separation between surface and deep ocean waters has been revised and is more consistent now. Extra details are now provided in the strongly extended Supplementary Information, which also includes extra graphs with relevant results. The discussion has been revised and manuscript now also includes a figure with C-13 isotopic profiles for different ocean basins. However, in some instances, the discussion of the results remains unnecessarily speculative: it should be possible to derive far more quantitative insight from the model results. The analysis of the results ought to go further than currently done. It is, e. g., incomprehensible that the diagnosed decoupling of the deepsea PO34- concentration from δ 13C and Δδ 13C in the Southern Ocean nutrient depletion experiment is not analysed any further. I encourage the authors to better make out the reasons for this decoupling, because, as they – correctly –it offers an alternative to the usual proxy interpretation of deviations from the δ 13C:PO3− 4 relationship. Finally, there are several troublesome errors in the paper. It is impossible that the weathering input of DIC has an average δ 13C signature of 14 ‰; it is also impossible for the ocean to degas CO2 where the surface ocean pCO2 is lower than pCOatm; figures document CO2 exchange fluxes in ice-covered regions, whereas the text states that ice cover blocks gas exchange. Please find details in the Specific Comments below. Given these fundamental errors and inconsistencies in the paper — which unfortunately shed doubt on the validity of the rest of the paper as well — I cannot but ask for another major revision.

Author response to Comment 1.2)

Thank you for again taking the time to thoroughly review our manuscript. We added more quantitative descriptions of our results throughout the manuscript. We extended our discussion of the Vmax experiment (the $\delta^{13}C$:PO_4^{3-} deviation), see our reply to referee comment 2.2.2 for more details. The weathering signature of $\delta^{13}C$ is revised (details given in our reply to referee comment 2.1.1) and the air-sea pCO_2 difference figure (original Fig. S3, now Fig. S4) is corrected (details in our reply to referee comment 2.1.2) after we were made aware of the discrepancy between original Fig. S3 and S4. The text on light and gas penetration through sea ice now better describes the difference between the model treatment of light and gas inhibition through sea ice (Sect. 2 as well as 3.3.4). We also provided more quantitative information such as fluxes in section 3.3.1, see our reply to referee comment 2.2.1 for more details.

Author's changes in the manuscript in response to Comment 1.2)

As described in detail in our reply to the specific comments below

Comment 2.1) Model calibration/spinup and control state

2.1.1 $\delta^{13}C$ of weathering DIC input

In the manuscript (page 4, line 7 and also in the response to Comment 2.2.3), we read that "The 13C/12C ratio in the weathering flux would be equivalent to a δ 13C of DIC of 14‰." There is something wrong with this 14‰ value. It is first of all completely unrealistic. The total sedimentary carbon subject to continental weathering has an average δ 13C of −5‰; the most abundant carbonate source has a δ 13C of 1.8 ± 0.2‰ (Derry and France-Lanord, 1996). Second, at steady state, this input requires a sink (or a combination of sinks) with globally equivalent characteristics. There is however no realistic combination of carbonate and organic carbon sinks that could lead to such a high average δ 13C.

2.1.2 Control run: ocean-atmosphere pCO2 gradient and air-sea CO2 flux

There are contradictions in the reported results for air-sea exchange of CO2 in the control run: in Fig. S4 (Supplementary Information p. 4), we see that there is a tongue-shaped area extending into the Atlantic Ocean in the Northern Hemisphere where the air-sea-flux of CO2 is positive, while the pCO2oc − pCO2atm difference is negative there, as can be seen in Fig. S3. This is a big flaw. Please check this!

2.1.3 Description and experimental design

Although the description of the model spin-up procedure has been improved it still lacks many important details. Except for the carbon isotopic signature of the weathering flux, it is still not specified on what quantitative basis the weathering fluxes have been determined. We now read that there are weathering fluxes for DIC, alkalinity, phosphate and silica, and that these are fed in at a fixed stoichiometric ratio, but that is all that is provided as information (why not simply report de values of the fluxes?).

Author response to Comment 2.1)

2.1.1 The 14 ‰ value was a mistake in the calculation, and we corrected this to -11 ‰, besides elaborating in general on the weathering fluxes and making a comparison with observational estimates. The 14 ‰ value was never in the model, so results are not affected. The new text describes that weathering fluxes are added homogeneously over the first ocean layer as dissolved matter and in a fixed stoichiometric ratio for $CaCO_3$, organic carbon, PO_4^{3-}, Alkalinity, and Si. Annual weathering fluxes (Tmol) are 27 for $CaCO_3$, 5 for organic carbon, 5/122 for PO_4^{3-}, 2*$CaCO_3$-16* PO_4^{3-} for Alkalinity, and 4.5 for Si. These values are within the uncertainties of observational estimates for Si (5.6 Tmol yr-1 (Tréguer, 2002)), $CaCO_3$ (~32 Tmol yr-1 (Milliman et al., 1996)), and organic carbon (4 Tmol yr-1 (Broecker and Peng, 1987)), and have been adjusted to improve the fit of the respective modelled marine tracer distributions as well as burial fluxes to observational estimates.

2.1.2 We thank the reviewer for spotting this, comparison of original figures S3 and S4 is indeed ground for confusion for any potential reader. The model results were correct, and we found that the mismatch between original Figures S3 and S4 was caused by a plotting error in making the original Fig. S3. The values reported in the text and analysis are not affected by this, so we expect that our replacement of Fig. S3 to a correct version (Fig. S4) will take away your concerns. We also added two extra subfigures to Fig. S4, for the gas exchange rate experiments, to clarify that section.

2.1.3. We extended the Methods section to include the stoichiometric ratios, the absolute fluxes in Tmol, and a comparison with observational estimates to improve the description of the weathering fluxes. See our response to comment 2.1.1.

Author's changes in the manuscript in response to Comment 2.1)

2.1.1 and 2.1.3: See changes in the text in Section 2
2.1.2: Fig. S3 replaced by correct version (Fig. S4), and extended to include gas exchange rate experiments

Comment 2.2) Results and discussion

Comment 2.2.1 Air-sea gas exchange rate experiments
This section remains one of the weakest of the study. Some parts are formulated in a vague qualitative style and provide little quantitative information (page 4, lines 5–20); others are long-winding, difficult to read and understand (page 4, lines 21–31). All in all the presentation and discussion of the results remain superficial and give an impression of a half-done job. First of all, the pCO2atm results presented in this section are to some extent counter-intuitive: increasing the gas exchange rate makes pCO2atm increase; reducing the same rate makes pCO2atm increase as well. In general, common sense would expect that opposite changes of the value of a model parameter lead to opposite effects, possibly except with strongly non-linear models; but even with non-linear models, this expectation should be met for sufficiently small perturbations of parameter values, except in very peculiar situations. A factor of four change can probably not be considered a small variation, so some non-linear behaviour has to be expected. In any case, I would consider deviations from this global scheme very suspect and would proceed to an in-depth analysis, starting with smaller perturbations (e.g., 50%, a factor of two) – finally there is no compelling reason for the particular choice of a factor of four. Here, these striking results are reported without any further ado. Strange enough, δ13Catm appears to behave as expected: increasing the gas exchange rate reduces δ13Catm; decreasing gas exchange rates increases δ13C atm.
Second, the discussion and analysis of the results consider only one half of the situation. The pCO2atm increase at increased gas exchange rates is ascribed to a weaker Southern Ocean carbon sink. Unfortunately, not a single quantitative flux value is given to support this claim! Let us apply the reasoning to the rest of the world, following the same logic. At steady state (or, after 2000 years of simulation, at quasi steady-state), the global net exchange of CO2 between the atmosphere and the ocean must be zero. If the perturbation experiment results present a weaker carbon sink Southern Ocean than the control run, it should also present a weaker carbon source elsewhere, most likely at low latitude. Following the same logic as before, a weaker carbon source to the atmosphere would be responsible for a lower pCO2atm. The conclusions that can be drawn from the kind of semi-qualitative argument that this discussion is based upon thus appear to be ambiguous, i. e., useless. Or there could be a stronger sink elsewhere (not mentioned though). Looking at sources and sinks is probably not the most reliable way to make out the mechanisms at work. What is sure, though, is that the global net exchange of CO2 between the ocean and the atmosphere is zero at steady state. Assuming a globally uniform pCO2atm, we then have

$$\sum_{i,j} A_{ij}(k_w)_{ij}(pCO_2^{atm} - (pCO_2^{oc})_{ij}) = 0 \qquad (1)$$

where i and j denumber the grid elements, Aij is the surface area and (kw)ij the specific gas exchange coefficient at grid point (i, j). Accordingly,

$$pCO_2^{atm} = \frac{\sum_{i,j} A_{ij}(k_w)_{ij}(pCO_2^{oc}{}_{ij})}{\sum_{i,j} A_{ij}(k_w)_{ij}}. \qquad (2)$$

This holds as is for steady state under any of the air-sea exchange experiments with globally perturbed (kw)ij 's: if these are uniformly increased by a factor of 4 (or any other value), that value cancels out. The key to understanding the pCO2atm changes lies thus in the distribution of pCO2oc, which in turn depends on the distribution of DIC and TA (assuming constant temperature and salinity). Gas exchange perturbations should have negligible impact on the TA distribution as long as the ocean-sediment exchange has not started to respond. So, it would be instructive to analyse how the surface ocean DIC distribution has changed. Third, referring in this context to Fig. S4 to support the reduced Southern Ocean sink argument adds further confusion and is to some extent misleading. In Fig. S4 ice cover has not been taken into account! This is really a terrible shortcoming of that figure! As stated elsewhere in the text, the Southern Ocean south of 60 °S is permanently covered by ice, which completely blocks gas exchange. The green band in the Southern Ocean has actually no meaning (it should actually not be there). In the Southern Ocean north of 60 °S I am, unfortunately, not able to make out any significant differences between the exchange rates of CO2 in the three panels. The total SO sink of atmospheric CO2 appears to be quite stable to me—please feel free to prove me wrong, with adequate flux numbers, which could certainly be easily derived from the model results. I do, however, see marked differences at low latitudes and they should be quantified in the discussion (e.g., integrated over a zonal band in the basin). And, by the way, it is not clear to me why Fig. S4 represents the situation after 100 instead of 2000 years.

To shed light on this confused situation, I have done some simulation experiments on my own with an ocean carbon cycle model, albeit of lower complexity than HAMOCC2s. First, I have performed a 120,000 yr control run, which was then continued by two 50,000 yr perturbation runs, mimicking fast gas and slow gas (using perturbations of the gas exchange constant by a factor of four). For what the results are worth and as food for thought, here is a summary of the results:

	after 2,000 yr			after 50,000 yr		
Experiment	pCO_2^{atm}	$\delta^{13}C^{atm}$	$\delta^{13}C^{avg}$	pCO_2^{atm}	$\delta^{13}C^{atm}$	$\delta^{13}C^{avg}$
Gas slow (/4)	289.4	−6.14	0.24	290.5	−6.29	0.15
Control	282.4	−6.53	0.25	282.4	−6.53	0.25
Gas fast (×4)	278.4	−6.77	0.26	277.7	−6.63	0.39

pCO_2^{atm} is reported in ppm and $\delta^{13}C$ in ‰; $\delta^{13}C^{avg}$ is the ocean-atmosphere average $\delta^{13}C$; control run extended at steady-state.

As expected, opposite perturbations of the rate constant produce effects in opposite directions. After 2,000 years, about 80% of the pCOatm 2 difference to 50,000 years is reached. There is some significant change in δ 13C atm beyond 2000 years, related to global ocean δ 13C adjustments towards the new steady state: in the gas-fast experiment, low-latitude surface ocean δ 13C is reduced by 0.23–0.26 ‰ after 2,000 years, leading to the burial of carbon with lower δ 13C than at the end of the control run, and thus gradually increasing the system average δ 13C. In the gas-slow experiment, the opposite happens (after 2,000 years, the low latitude surface ocean δ 13C is increased by 0.1–0.2 ‰, and as result of burial changes global ocean δ 13C decreases). I would really recommend to run all of the experiments far beyond 2000 years. So many interesting things happen once the sediment feedback is allowed to come into play. . .

Author response to Comment 2.2.1)

Thank you for your elaborate comment on the air-sea gas exchange section, and helping us to understand remaining problems with this section. We discovered a problem in the gas exchange routine in the model that explains the absence of a divergence of pCO2 in the gas fast vs. gas slow experiments: The gas exchange routine was corrected for giving better convergence for the computation of the first guess value of pCO2 at the new time step (Due to the time step of one year, one needs to use an average of the pCO_2 from the old time step and an extrapolation of pCO_2 at the new time step for potential full

equilibration with the atmospheric pCO_2 -There was a bug in the original scheme for this extrapolation). With this modification, the correct – small – atmospheric pCO_2 variation for lowered gas transfer velocity is now also achieved. All model runs have been repeated with this modification to be fully consistent with each other. All Figures and values have thus been updated throughout the text. As you can see, the differences are small, and have had no effect on any conclusions involving (the vertical gradient of) $\delta^{13}C$, the main topic of our study. Importantly, the results for pCO_2 are now diverging for the gas exchange experiments, which is to be expected from the experiments - as the reviewer argued.

We rewrote the air-sea gas exchange section to clarify the points raised in reviewer comment 2.2.1 and 2.1.2. We added values for the air-sea fluxes wherever relevant, or gave the change relative to the control run as a percentage if this aids readability. Our description is supported by an extended Fig. S4 for the pCO_2 gradient across the air-sea interface. Our choice of a factor 4 is reasoned for in the text in the last sentence of the first paragraph of section 3.3.1. In equilibrium, global net exchange is indeed zero as described in Eq. (1) in the reviewer comment 2.2.1, but pCO_2 changes only in the transient phase when Eq. (1) is non-zero - which happens in approximately the first 600 years as visible from Fig. S3. This is also why we initially presented results (in for example the original Fig. S4) during the transient phase at 100 years. As this clearly led to confusion, we removed the original Fig. S4 from the SI (but still provide it here in our reply, see our response to Comment 3) and restricted the section to describing 2000 year results. Also, note that the air-sea pCO_2 difference figure shows the combined result of the change in surface ocean pCO_2 and atmospheric pCO_2. We clarified the presence of a small air-sea C flux through the sea ice by extending the methods description: Here, we included the difference between light (full inhibition when ice is present) and gas transfer (partial inhibition depending on sea ice thickness). The green band in the original Fig. S4 thus had a meaning, as there is a (very) small flux through the ice, because the air-sea gas exchange rate is scaled by division through the ice thickness in cm and thus never fully becomes zero.

The duration of the sensitivity experiments is kept at 2000 years, for which we give a series of reasons: The most important one is that the main response to the applied change occurs within the first few hundred years of the experiment (as visible in Fig. S3). We performed a 50 000 year run for the Gas Fast experiment and compared the results to our previous 2000 year results, and indeed see an additional drift in atmospheric $\delta^{13}C$ and pCO_2 over these additional 48 000 years - of similar size to what the reviewer has presented us for his or her model. Another major reason for not continuing the experiments beyond 2000 years (except for the already presented 12000 year POC fast experiment) is that the calculated $\Delta\delta^{13}C$ is already equilibrated after 2000 years (no difference between 2000 and 50000 year result), and $\Delta\delta^{13}C$ is the topic of our study. Besides that, other processes would come into play on such long timescales as already argued in the first paragraph of section 3.3.2. A final argument against doing longer experiments is that choosing an experiment duration of for example 50 000 years would still not be enough to equilibrate $\delta^{13}C$ (as mentioned in the text and shown by Roth et al. (2014) who had a continuing $\delta^{13}C$ drift beyond 200 000 years). One should thus consider any $\delta^{13}C$ distribution to be only in quasi-equilibrium, and we choose the 2000-year $\delta^{13}C$ distribution (that has incorporated its main initial, 'fast', response to our perturbations). We stressed this by adding the word 'quasi-equilibrium' in the Methods experiment description and in several other places where it is relevant, and by extending the caption of Fig. S3.

We tested smaller perturbations of the gas exchange rate as well. The effects are as expected smaller (and diverging, from the corrected gas exchange routine). We however choose to present the more extreme cases of a very high (4x) and low (division by 4) gas exchange rate in the text: We do this in order to show the reader the potential effects of bringing surface ocean $\delta^{13}C$ very far away or very close to its equilibrium with the atmosphere – stressing the contrast between low and high latitudes.

Comment 2.2) Results and discussion

Comment 2.2.2 The biological pump: SO nutrient depletion
On page 10 (lines 14–17) we read that This is interesting in light of glacial proxy interpretation, as deviations from the δ 13C:PO3− 4 relationship (Sect. 2) are usually interpreted as the influence of air-sea gas exchange on δ 13C (Eide et al., 2017b; Lear et al., 2016), but could thus also come from changes in nutrient uptake efficiency. As for a changed POC sinking rate, Δδ13C is affected more in older waters (Fig. 4). This is not only interesting. I would rate this as the most important outcome of this study. It is, unfortunately, not followed any further. No attempt is made to analyse this decoupling and to work out the contributing mechanisms.

Author response to Comment 2.2.2)

We understand the need for a more elaborate explanation on this aspect. In order to clarify our statements, we have adjusted the precision of language in this part of Sect. 3.3.3 and provided a new Figure on the relationship between PO_4^{3-} and $\delta^{13}C$ in the different experiments (Fig. 8). From this new figure, it is visible that both changes in air-sea gas exchange and changes in biological uptake in the SO can change the global goodness-of-fit to the $\delta^{13}C$:PO_4^{3-} relationship. The fit thus depends on the relative importance of biology and air-sea gas exchange (see also Fig. 2) – and should not be interpreted as the influence of air-sea gas exchange on $\delta^{13}C$ alone (as has been done before). The sentence 'As for a changed POC sinking rate, $\Delta\delta^{13}C$ is affected more in older waters (Fig. 4)' has no connection to the deviations from the $\delta^{13}C$: PO_4^{3-}relationship (as this relationship does not consider the vertical gradient of $\delta^{13}C$), and is moved to improve readability.

Author's changes in the manuscript in response to Comment 2.2)

2.2.1 Section 3.3.1 is rewritten in response to the concerns raised by the referee and editor. We also updated all figures and values in the text because all model runs had to be redone after finding a problem with the gas exchange routine (see details in our reply to comment 2.2.1). Besides that, extra text on sea ice gas and light inhibition is added to the Methods in Sect. 2.

2.2.2 We elaborated in Sect. 3.3.3 on the deviation from the $\delta^{13}C$:PO_4^{3-}relationship, by providing extra text and adding a new figure showing this relationship for a selection of experiments.

Comment 2.3) Supplementary Information

As mentioned in section 2.1.2 above, there are problems with the model results reported in Figs. S3 and S4. Please check this.

Author response to Comment 2.3)

See our reply to comment 2.1.2.

Author's changes in the manuscript in response to Comment 2.3)

See our reply to comment 2.1.2.

Comment 3) Technical comments

Thank you for noting these technical mistakes. We added our reply to the comments directly below each comment in italicised text in order to improve readability of our corrections.

Manuscript

Throughout the paper: please use the verb "to lower" (and similarly "to reduce" with a positive amount (e.g., "to lower by 1‰", not "to lower by −1‰").

Corrected throughout manuscript

Page 1, line 8: please add the reference for the standard ratio (Craig, 1957).

Added in text and to reference list

Page 2, line 17: please explain what a "free box atmosphere" is

Rephrased to 'a one-layer atmosphere component assumed to be longitudinally well-mixed' to clarify and updated SI1B to match this adjustment

Page 3, line 30: the correct units for temperature in the parametrization for eta are "K" not "°C" (try to apply it at 0°C...)

Corrected to K

Page 5, line 11: strange sentence construction. I suggest to rephrase as "[. . .] we express δ 13Cbio as a percentage (denoted δ 13C perc bio because [. . .]"

Sentence revised

Page 5, line 16: the absolute values are superfluous as both Fup and Fdown are positive (cf. SI 1B, and also Heinze and Maier-Reimer (1999))

We agree that these can be removed, the manuscript has been adjusted accordingly

Page 5, line 18: Fnet should be defined as Fnet = Fup − Fdown (cf. SI 1B, and also Heinze and Maier-Reimer (1999))

This is indeed clearer, our analysis had negative downward fluxes which explained the absolute sign and the Fnet=Fup + Fdown, but now the presentation is clearer and more consistent. Thank you for drawing our attention to this.

Page 6, line 25: replace "results in room" by "leaves room"

Corrected as suggested

Page 6, line 27: replace "times slower" by "times more slowly"

Corrected as suggested

Page 7, line 11: "(Fig. S4 and 5)" should probably read "(Fig. S4 and S5)"

Corrected

Page 7, line 17: the sentence "Slow gas exchange reduces Fu+d causing less fractionation to occur. . . " does not really make sense. Fractionation is dependent on temperature, which remains unchanged. The contrast or the difference between air and sea is changed, because the air-sea-exchange fluxes play a lesser role in the surface ocean 13C balance allowing a greater difference between atmosphere and ocean. Please rewrite.

We see how a reader can misinterpret this sentence as it is not precise, and we have rewritten to increase clarity.

Page 8, line 25: "can be"? is it or is it not? If it is, say "is", else please discuss!

Replaced by 'is'

Page 9, line 2: replace "is more confined to" by "is confined closer to"

Corrected as suggested

Page 9, line 27: "probably"? Why speculate? The model results should allow to verify this.

Corrected

Page 10, line 11: replace “(up to −0.8‰)” by “(by up to 0.8‰)”

Corrected as suggested

Page 11, line 5: “course” should read “source” Page 11, line 6: replace “earlier” by “previously”

Corrected as suggested

Page 11, line 10: Fig. S6 relates to the slow gas experiment. Not sure this is the one to refer to here.

The sign of the change in the Gas Slow experiments equals the sign of the disequilibrium, as mentioned in the caption of Fig. S6. We nevertheless removed the reference to Fig. S6 because we see how it can be confusing when referred to in this section on sea ice.

Page 11, line 13: replace “with” by “by”

Corrected as suggested

Page 11, line 27: replace “advance” by “spread” or “extend”

Corrected

Page 11, line 28: replace “increased up to” by “increased by up to”

Corrected as suggested

Page 12, line 1: replace “varies up to ∼±0.4‰” by “varies by up to about ±0.4‰” (do not place two symbols immediately one after the other)

Corrected and also corrected other occurrences of double symbol use throughout the manuscript

Page 13, line 19: replace “varies up to ∼±0.5‰” by “varies by up to about ±0.5‰”

Corrected as suggested

Page 13, line 21: “is important” should read “are important”

Corrected as suggested

Supplementary Information

Page 2: there is much confusion and there are several errors in this paragraph. To bring it in line with the graphs, the model documentation (Heinze and MaierReimer, 1999) and the main paper, it needs to be corrected as follows: • Fup = kw ∗ [A]water • Fdown = kw ∗ [A]air • FA = kw ∗ ([A]water − [A]air)

Corrected to be in line with the rest of the manuscript, as suggested.

Page 4, caption to Fig. S3: what exactly is meant by “Negative values indicate a potential carbon flux to the ocean?” Why “potential”?

Clarified in the caption.

Page 4, caption to Fig. S4: not sure what the integrated fluxes are meant to tell. Is there something special after 100 years? We try to understand the state after 2000 years. Why is the state after 2000 years not shown here instead?

The globally integrated C flux through the air-sea interface will increase or decrease pCO_2 during the transient phase, depending on its sign. After reaching equilibrium, the globally integrated C flux is (very close to) zero, as described in equation (1) presented by reviewer in their report. Atmospheric pCO_2 changes only during the transient phase where eq (1) is non-zero, and this effect is most pronounced after ~100 years, which explains our previous focus on this. As the discovery and solving of a problem with the air-sea gas exchange routine now results in the expected divergence of pCO_2, we decided to remove the 100-year figures and text. The focus of the manuscript is on $\delta^{13}C$, and we see the reader ‘sudden’ 100-year results confuse when the rest of the text is on 2000-year results. However, the updated figure (after rerunning the model with the corrected air-sea gas exchange routine) is given below in case the reviewer is interested:

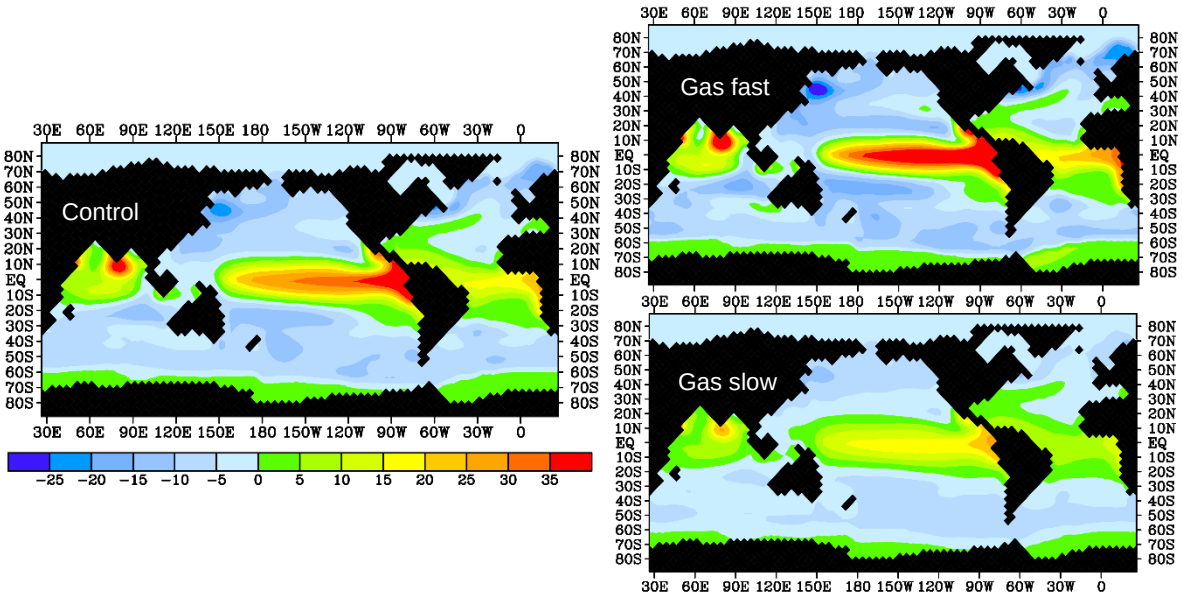

Page 4, Figs. S3 and S4: unfortunately, the colour scales chosen here are somewhat misleading. On Fig. S3, the rich green tone covers the first negative interval (i.e., the one next to 0) while on Fig. S4, it covers the first positive interval.

We corrected this in the new Fig. S4 so that both figures now have the first positive interval in green.

Page 5, Fig. S5: It would be best if all the figures had the same vertical axis extent. If this is not possible, at least graphs appearing side by side should have the same extents (both pCO_2 and δ 13C axes).

We adjusted the axes in new Fig. S3 a way that graphs appearing side by side now have the same pCO_2 and $\delta^{13}C$ axes.

Editor Comments) Summary of comments that come in addition to the above-presented referee comments

1. *Address apparent mismatch between Fig. S3 and S4*
2. *Compare weathering fluxes to data-based estimates*
3. *Rewrite section 3.3.1*
4. *Decide on simulation duration*
5. *Make figure captions more specific in Fig. 3 and following and provide information on time of results*
6. *Refer to equilibration timescale of* $\Delta\delta^{13}C$
7. *Page 6, line 19ff (of marked-up MS): The text on the equilibration time is not very precise and the explanation for the longer equilibration time scale of 13C compared to oxygen is in my opinion not correct. Probably you would like to address how long it takes to equilibrate the atmosphere and ocean surface layer by air-sea gas exchange (not considering surface-to-deep exchange) for O2, DIC, and 13C(DIC) after a small perturbation in surface ocean O2, DIC and* $\delta^{13}C$*(DIC), respectively. The equilibration time depends on how fast the tracer amount in the surface layer is replaced by air-sea gas exchange as further moderated by the Revelle factor for DIC.*

   (For this you may solve the according differential equations:
   d/dt x(s) = F(x(s), x(a)) and d/dt x(a) = - F(x(s), x(a))

to extract the exponential time scale associated with the re-equilibration. F is the net air to sea flux and x(s) and x(a) the perturbation in the atm. and surface layer))

8. *p6, line 25: suggest to delete this sentence as unclear and not precise. (The surface ocean $\delta^{13}C$ is not in equilibrium with the atmosphere in many region due to the slow equilibration time scale for $\delta^{13}C$ with respect to gas exchange with the atmosphere.)*
9. *p6, line 29: It is highly misleading to state that air-sea equilibrium would be 2 ‰ as the equilibrium depends strongly on temperature and varies greatly with latitude*

Author response and changes in the manuscript in response to Editor Comments)

1. The mismatch between Fig. S3 and S4 was caused by a plotting error in making Fig. S3, we replaced this figure (new Fig. S4) as described in our response to referee comment 2.1.2. The model results were correct, and the text and conclusions are therefore unaffected by this change.
2. The text on the weathering fluxes has been extended as described in our reply to referee comment 2.1.1
3. We thoroughly revised the text on the air-sea gas exchange experiment, making it more precise, adding more quantitative information and providing more support for our results (extended Fig. S4 as compared to original Fig. S3). While addressing the issue with the air-sea gas exchange experiments, we found a problem in the air-sea gas exchange routine of the model. We solved this problem and re-ran all model experiments with the correct air-sea gas exchange routine – See our reply to reviewer comment 2.2.1 for details.
4. We decided to keep our experiment duration at 2000 years, and give a lists of arguments in our reply to referee comment 2.2.1
5. Captions adjusted to include that all figures are 2000-year differences. The captions of the difference plots now also have a more uniform format
6. This is now referred to in Sect. 2
7. We included a revision of this paragraph in our general revision of section 3.3.1. We provide the reader with quantitative estimates of the equilibration times (from Jones et al., 2014) and stress that we discuss the equilibration timescale through the air-sea interface. We now describe the contrast between CO_2 (for which equilibration depends on the Revelle Buffer factor) and the $^{13}CO_2/^{12}CO_2$ ratio (which is not facilitated by the buffering reaction of CO_2 with H_2O but scales by the DIC:CO_2 ratio, see the text and Galbraith et al., 2015).
8. We agree that the use of the word equilibrium is misleading when discussing $\delta^{13}C$. We therefore removed the second part of sentence in order to keep the information of small carbon outgassing in the manuscript.
9. The original text was meant to describe average equilibrated $\delta^{13}C_{surface}$, which is approximately 2 ‰ (Murnane and Sarmiento, 2000), since $\delta^{13}C^{atm}$ is about -6.5 ‰ and mean air-sea fractionation about 8.5 ‰ (Mook et al., 1986). $\delta^{13}C_{surface}$ is however indeed strongly dependent on temperature, and we therefore adjusted the text to clarify the latitudinal contrasts. We also added information on the model-specific temperature effects on air-sea fractionation.

Marked-up manuscript

See remainder of this document.

Southern Ocean controls of the vertical marine $\delta^{13}C$ gradient – a modelling study

Anne L. Morée[1], Jörg Schwinger[2], Christoph Heinze[12]

[1]Geophysical Institute, University of Bergen, Bjerknes Centre for Climate Research, 5007 Bergen, Norway
[2]Uni Research Climate, Bjerknes Centre for Climate Research, 5007 Bergen, Norway

Correspondence to: Anne L. Morée (anne.moree@uib.no)

Abstract. $\delta^{13}C$, the standardised $^{13}C/^{12}C$ ratio expressed in permil, is a widely used ocean tracer to study changes in ocean circulation, water mass ventilation, atmospheric pCO_2 and the biological carbon pump on timescales ranging from decades to tens of millions of years. $\delta^{13}C$ data derived from ocean sediment core analysis provide information on $\delta^{13}C$ of dissolved inorganic carbon and the vertical $\delta^{13}C$ gradient (i.e., $\Delta\delta^{13}C$) in past oceans. In order to correctly interpret $\delta^{13}C$ and $\Delta\delta^{13}C$ variations, a good understanding is needed of the influence from ocean circulation, air-sea gas exchange and biological productivity on these variations. The Southern Ocean is a key region for these processes, and we show here that $\Delta\delta^{13}C$ in all ocean basins is sensitive to changes in the biogeochemical state of the Southern Ocean. We conduct a set of idealised sensitivity experiments with the ocean biogeochemistry general circulation model HAMOCC2s to explore the effect of biogeochemical state changes of the Southern and Global Ocean on atmospheric $\delta^{13}C$, pCO_2, and marine $\delta^{13}C$ and $\Delta\delta^{13}C$. The experiments cover changes in air-sea gas exchange rates, particulate organic carbon sinking rates, sea ice cover, and nutrient uptake efficiency - in an unchanged ocean circulation field. Our experiments show~~We conclude~~ that global mean $\Delta\delta^{13}C$ varies by up to about ±0.35 ‰ around the pre-industrial model reference (1.2 ‰) in response to biogeochemical change.~~the maximum variation of mean marine $\Delta\delta^{13}C$ in response to biogeochemical change is ~±0.4 ‰. However, t~~ The amplitude of this sensitivity can be ~~higher~~ larger at smaller scales, as seen from a maximum sensitivity of about ~~~-0.6 ‰ on ocean basin scale. The ocean's oldest water (North Pacific) responds most to biological changes, the young deep water (North Atlantic) responds strongly to air-sea gas exchange changes, and the vertically well-mixed water (SO) has a low or even reversed $\Delta\delta^{13}C$ sensitivity as compared to the other basins. This local $\Delta\delta^{13}C$ sensitivity depends on the local ~~prior~~ thermodynamic disequilibrium and the $\Delta\delta^{13}C$ sensitivity ~~of~~ to local POC export production changes~~to biogeochemical change~~. ~~Interestingly, t~~The direction of both glacial (intensification of $\Delta\delta^{13}C$) and interglacial (weakening of $\Delta\delta^{13}C$) $\Delta\delta^{13}C$ change matches the direction of the sensitivity of biogeochemical processes associated with these periods. ~~T~~ This supports the idea that biogeochemistry likely explains part of the reconstructed variations in $\Delta\delta^{13}C$, in addition to changes in ocean circulation.

1 Introduction

The vertical marine $\delta^{13}C$ gradient ($\Delta\delta^{13}C$) is the surface-to-deep difference in $\delta^{13}C$ of dissolved inorganic carbon (DIC), where the standardised $^{13}C/^{12}C$ ratio ($\delta^{13}C$) is expressed in permil (Zeebe and Wolf-Gladrow, 2001):

$$\delta^{13}C = \left(\frac{^{13}C/^{12}C}{(^{13}C/^{12}C)_{standard}} - 1\right) * 1000\ ‰. \quad (1)$$

Here, $^{13}C/^{12}C_{standard}$ is the Pee Dee Belemnite standard (0.0112372) (Craig, 1957). ^{13}C is slightly heavier than the ^{12}C isotope which causes a fractionation effect during air-sea gas exchange and photosynthesis, thereby changing $\delta^{13}C$ and $\Delta\delta^{13}C$ (Laws et al., 1997; Mackenzie and Lerman, 2006; Zhang et al., 1995). Photosynthetic fractionation increases the $^{13}C/^{12}C$ ratio of surface ocean DIC (i.e., a $\delta^{13}C$ increase) due to the preferred uptake of the lighter ^{12}C into biogenic matter (which therefore has a low $\delta^{13}C$). The deep sea DIC has a relatively low $\delta^{13}C$ signature as a result of the remineralisation of low-$\delta^{13}C$ biogenic matter at depth. The resulting vertical $\delta^{13}C$ gradient is in addition influenced by air-sea gas exchange and circulation (Emerson and Hedges, 2008; Zeebe and Wolf-Gladrow, 2001; Ziegler et al., 2013). Both deep sea and surface ocean $\delta^{13}C$ signatures are archived in the calcareous shells of foraminifera in the sediments. Such ~~R~~records of $\delta^{13}C$ from planktic and benthic foraminiferal shell material cover tens of millions of years (Hilting et al., 2008). Using this archive, $\delta^{13}C$ and $\Delta\delta^{13}C$ have been used to reconstruct for example atmospheric CO_2 concentration, ocean circulation and the strength of the biological pump (Bauska et al., 2016; Broecker, 1982; Broecker and McGee, 2013; Crucifix, 2005; Curry and Oppo, 2005; Hollander and McKenzie, 1991; Hoogakker et al., 2015; Keir, 1991; Lisiecki, 2010; Oppo et al., 1990; Shackleton and Pisias, 1985; Zahn et al., 1986; Ziegler et al., 2013). ~~Note that~~ $\Delta\delta^{13}C$ is independent of whole-ocean $\delta^{13}C$ shifts (due to terrestrial influences), because such influences would affect $\delta^{13}C$ equally everywhere. ~~, t~~ This~~herefore~~ mak~~es~~~~ing~~ $\Delta\delta^{13}C$ ~~it~~ a valuable proxy to study the marine carbon cycle independent of changes in carbon storage on land. Besides the use of $\delta^{13}C$ for understanding the past ocean, ~~C~~contemporary measurements of $\delta^{13}C$ of DIC support the quantification of anthropogenic carbon uptake by the oceans as well as the study of the effects of biology and ocean circulation on tracer distributions (Eide et al., 2017b; Gruber and Keeling, 2001; Holden et al., 2013; Kroopnick, 1980; Kroopnick, 1985; Quay et al., 2003). However, major uncertainties remain in the interpretation of foraminiferal $\delta^{13}C$ records and $\Delta\delta^{13}C$ (Broecker and McGee, 2013; Oliver et al., 2010) as well as in the interpretation of the present day $\delta^{13}C$ data (Eide et al., 2017b).

This article addresses part of these uncertainties by exploring the pre-industrial sensitivity of $\delta^{13}C$ and $\Delta\delta^{13}C$ to biogeochemical change in idealised model experiments. By doing so we can investigate a number of biogeochemical mechanisms that could explain (part of) the observed changes in $\delta^{13}C$ and $\Delta\delta^{13}C$. We focus on the Southern Ocean (SO), the ocean south of 45° S, because the SO plays an important role in the global carbon cycle by regulating atmospheric CO_2 concentrations and uptake of anthropogenic CO_2 (Broecker and Maier-Reimer, 1992; Heinze, 2002; Marinov et al., 2006) as well as influencing the global efficiency of the biological pump, global primary production and preformed nutrients (Primeau et al., 2013).

Variations in $\Delta\delta^{13}C$ over the past few 100 000 years show that $\Delta\delta^{13}C$ is generally increased during glacial periods, due to a higher contrast of deep $\delta^{13}C$ with surface and mid-depth $\delta^{13}C$ (Broecker, 1982; Boyle, 1988; Charles et al., 2010; Oliver et al., 2010; Shackleton and Pisias, 1985). Long-term $\delta^{13}C$ and $\Delta\delta^{13}C$ variations have been explained by ocean circulation changes

(Duplessy et al., 1988; Jansen, 2017; Oppo et al., 1990; Toggweiler, 1999; Menviel et al., 2016). However, $\Delta\delta^{13}C$ variability cannot be explained by ocean stratification/circulation changes alone: An interaction between biogeochemical and physical processes must be at play (Boyle, 1988; Charles et al., 2010; Keir, 1991; Mulitza et al., 1998; Schmittner and Somes, 2016; Ziegler et al., 2013). $\Delta\delta^{13}C$ has been used in different ways over time: In earlier studies as the contrast between surface and deep water $\delta^{13}C$, derived from planktic versus benthic foraminifera (Boyle, 1988; Broecker, 1982; Duplessy et al., 1988; Shackleton et al., 1983) and now increasingly as the contrast of deep ocean (benthic) $\delta^{13}C$ with thermocline or intermediate ocean $\delta^{13}C$ (Charles et al., 2010; Lisiecki, 2010; Mulitza et al., 1998).

Here, we explore the sensitivity of $\delta^{13}C$ and $\Delta\delta^{13}C$ to changes in the biogeochemical state of the Global Ocean and Southern Ocean under a constant circulation field, to support the paleo-oceanographic interpretation of $\delta^{13}C$ and $\Delta\delta^{13}C$ as well as to improve the understanding of the SO role in global carbon cycling and its variability and sensitivity. In order to study biogeochemical mechanisms that could influence $\delta^{13}C$ and $\Delta\delta^{13}C$, a set of sensitivity experiments is conducted with the ocean biogeochemistry general circulation model HAMOCC2s (Heinze et al., 2016). We first estimate the contribution of biology versus air-sea gas exchange to marine $\delta^{13}C$ of DIC (Sect. 3.2). The experiments focus on one or more of the biogeochemical aspects assumed to be important for $\delta^{13}C$ and $\Delta\delta^{13}C$, e.g. the biological pump efficiency and/or equilibration at the air-sea interface (Sect. 3.3.1-3.3.4). Together these experiments provide a broad spectrum of biogeochemical changes that could influence local and global $\delta^{13}C$ and $\Delta\delta^{13}C$. The modelling results of Sect. 3.3.1-3.3.4 are discussed in context of observational data from sediment cores (Sect. 3.4). As $\delta^{13}C$ and $\Delta\delta^{13}C$ are used to study changes in atmospheric pCO_2 (pCO_2^{atm}), a final section will cover the relationship between atmospheric $\delta^{13}C$, $\Delta\delta^{13}C$ and pCO_2^{atm} under different marine biogeochemical states (Sect. 3.5).

2 Methods

In this study we employ the ocean biogeochemistry general circulation model HAMOCC2s (Heinze et al., 1999; Heinze et al., 2009; Heinze et al., 2016) which simulates the inorganic and organic carbon cycle in the water column and in the sediments. The horizontal resolution of the model is 3.5° × 3.5° and there are 11 depth layers in the ocean. HAMOCC2s has an annual time step and an annually averaged fixed circulation field, as well as a ~~free~~one-layer ~~box~~ atmosphere component (permitting exchange of O_2, $^{13}CO_2$ and CO_2 with the ocean component) which is assumed to be longitudinally well-mixed~~ere for O_2, $^{13}CO_2$ and CO_2~~. The model is computationally very economic and thus an ideal tool for sensitivity experiments over long integration times. Biogenic particulate matter in the model is represented as particulate organic carbon (POC), calcium carbonate ($CaCO_3$) and biogenic silica (opal). These biogenic particles are only modelled as export production due to the annual time-step of the model. POC and opal export production are described by Michaelis-Menten kinetics for nutrient uptake, limited by phosphate and silicic acid respectively (SI 1A). $CaCO_3$ export production depends on the ratio between opal and POC production. POC is carried as a tracer as well as transported downwards according to a set of mass balance equations that describe POC gain through surface layer POC production and POC losses through constant sinking and remineralisation rates (SI 1A). This is

done similarly for opal and $CaCO_3$ sinking and dissolution. As the model has an annual time step, sea ice is always present south of ~60° S and north of ~70° N in the control run (Fig. S1). A more detailed model description is provided in previous studies using a similar configuration of HAMOCC2s (Heinze, 2002; Heinze et al., 2016), as well as in SI 1A.

Fractionation between~~d~~ ^{13}C and ^{12}C during photosynthesis is set to a constant value of -20 ‰ (Lynch-Stieglitz et al., 1995; Tagliabue and Bopp, 2008), as model results are little influenced by the chosen parameterisation (Jahn et al., 2015; Schmittner et al., 2013). The fractionation during air-sea gas exchange depends on temperature according to ε=-9.483*10^3/T [K~~° C~~] + 23.89 ‰ (Mook, 1986), causing stronger fractionation at lower temperatures (i.e. at high latitudes). Fractionation during $CaCO_3$ formation is omitted from the model as done in previous studies (Lynch-Stieglitz et al., 1995; Marchal et al., 1998; Schmittner et al., 2013), as its size is uncertain but likely minor (~1 ‰) and effects on $\delta^{13}C$ and $\Delta\delta^{13}C$ are small (Shackleton and Pisias, 1985). In the version of HAMOCC2s used in this study, a fixed weathering input is used for ^{13}C to tune the ocean inventory to values comparable to observations. The weathering flux of ^{13}C into the ocean was determined by an iterative procedure:

The model was run over 100,000 years replacing the weathering rate with the diagnosed burial rate for ^{13}C continuously. After this, the model ^{13}C inventory was recalibrated such that the atmospheric value for $\delta^{13}C$ arrived at -6.5 ‰. This procedure was repeated over three iterations. Afterwards, the weathering rate of ^{13}C was fixed to the last diagnosed value (0.36 Tmol ^{13}C yr^{-1}) – which results in a weathering flux $\delta^{13}C$ of DIC of -11 ‰. Another 100,000 yr run was carried out with this constant input rate in order to check whether the global ^{13}C distribution was stable in all reservoirs. The sensitivity experiments were then re-started from the result of that run.~~The 'best fit' weathering value was found by running the model with a restored atmosphere ($\delta^{13}C$= 6.5 ‰) until the prognostic burial rate and weathering flux equilibrated to a constant value F_{eq}^{w} (~110000 model years). Consecutively, atmospheric restoring was removed and the weathering rate for ^{13}C was fixed to value F_{eq}^{w} .~~ Weathering fluxes are added homogeneously over the first ocean layer as dissolved matter and in a fixed stoichiometric ratio for $CaCO_3$, organic carbon,~~C, O$_2$, Alkalinity,~~ PO_4^{3-}, Alkalinity, and Si. Annual weathering fluxes (Tmol) are 27 for $CaCO_3$, 5 for organic carbon, $5/r_{C:P}$ for PO_4^{3-}, 2*$CaCO_3$-$r_{N:P}$*PO_4^{3-} for Alkalinity, and 4.5 for Si (with $r_{C:P}$ = 122 and $r_{N:P}$ = 16). These values are within the uncertainties of observational estimates for Si (5.6 Tmol yr^{-1} (Tréguer, 2002)), $CaCO_3$ (~32 Tmol yr^{-1} (Milliman et al., 1996)), and organic carbon (4 Tmol yr^{-1} (Broecker and Peng, 1987)), and have been adjusted to improve the fit of the respective modelled marine tracer distributions as well as burial fluxes to observational estimates. ~~The $^{13}C/^{12}C$ ratio in the weathering flux would be equivalent to a $\delta^{13}C$ of DIC of 14 ‰.~~ The spinup procedure described here created a~~is procedure created a free atmosphere~~ model setup with close-to-observed marine and atmospheric $\delta^{13}C$ ($\delta^{13}C^{atm}$) values and freely evolving atmospheric pCO_2 and $\delta^{13}C$. This equilibrated model version is referred to as the 'control run' in the remainder of this article. We define the vertical $\delta^{13}C$ gradient ($\Delta\delta^{13}C$) as:

$$\Delta\delta^{13}C = \delta^{13}C_{surface} - \delta^{13}C_{deep}\ , \qquad (2)$$

where $\delta^{13}C_{surface}$ and $\delta^{13}C_{deep}$ are the volume-weighted mean $\delta^{13}C$ of DIC in the surface ocean (< 50 m depth, i.e. the model photic zone) and the deep ocean (lowermost wet layer in the model, if top of layer > 3 km depth), respectively. By doing so, we can compare the $\Delta\delta^{13}C$ summarised as one number between the different sensitivity experiments.

We conducted a set of sensitivity experiments to explore changes in air-sea gas exchange rate, sea ice extent (influencing both biological production and the air-sea gas exchange of carbon) and the efficiency of the biological pump through the POC sinking rate and nutrient uptake rate (Table 1). We employ the term 'efficiency of the biological pump' as a measure of the success of phytoplankton to maintain low nutrient concentrations in the surface ocean. All experiments are run for 2000 model years starting from the end of the spinup. These runtimes allowed for atmospheric quasi-equilibrium to establish (Fig S5~~4~~), with an exception for the long-term effects caused by POC sinking rate changes (as studied in more detail by Roth et al. (~~,~~ 2014)). The equilibration timescale of $\Delta\delta^{13}C$ is much shorter than that of atmospheric $\delta^{13}C$: This is the case because 1) the long-term weathering-burial equilibration of $\delta^{13}C$ affects the whole ocean reservoir simultaneously – thus keeping $\Delta\delta^{13}C$ constant and 2) the processes that potentially influence $\Delta\delta^{13}C$ (changes in biological production and air-sea gas exchange) affect $\Delta\delta^{13}C$ on shorter (centennial to millennial) timescales. In order to compare effects of SO change and Global change, ~~T~~the gas exchange rate and POC sinking rate experiments are done twice ~~-~~, once changing the respective model parameter for the Global Ocean and once for the Southern Ocean only (SO-only). The model parameters where changed in a way that marine biogeochemical tracer distributions (e.g. PO_4^{3-}, $\delta^{13}C$) remained reasonable but did provide an estimate of the sensitivity of the respective tracer to biogeochemical change. The model has a constant sea ice cover (Fig. S1), which permits gas ~~and light~~ transfer through the ice depending on ice cover ~~fraction~~thickness (the transfer rate is divided by ice thickness in cm) while light transfer is inhibited at ice thicknesses over 0.01 cm. The maximum and minimum sea ice cover experiments (Ice large and Ice small, Table 1) approximate the Last Glacial Maximum winter extent and the modern summer extent of SO sea ice, respectively (Crosta (2009) and Fig. A22 therein) and assume full inhibition of gas and light transfer through ice for simplicity. The experiment on nutrient drawdown (V_{max}) alters the Michaelis-Menten kinetics of POC production by changing the maximum nutrient (i.e. PO_4^{3-}) uptake rate (V_{max}^{POC} in SI 1A). The gas exchange experiments alter the specific gas exchange rate k_w as described in more detail in SI 1B. The POC sinking rate experiments change the sinking velocity constant w_{POC} in the POC mass balance equations (SI 1A).

The contribution of biological processes versus air-sea gas exchange to $\delta^{13}C$ is calculated using the method of Broecker and Maier-Reimer (1992) as done for observations by Eide et al. (2017b) and in a modelling context by Sonnerup and Quay (2012):

$$\delta^{13}C_{bio}[‰] = \frac{\varepsilon_{photo}}{\overline{DIC}} * r_{c:p} * (PO_4 - \overline{PO_4}) + \overline{\delta^{13}C}\ , \qquad (3)$$

where $\varepsilon_{photo} = -20\ ‰$, $r_{c:p} = 122$ and the following model control run mean values are used: $\overline{DIC} = 233208.284793\ \mu mol/kg$, $\overline{PO_4} = 2.409399\ \mu mol/kg$ and $\overline{\delta^{13}C} = 0.656742\ ‰$. These values result in the modelled $\delta^{13}C_{bio}$:PO_4^{3-} relationship $\delta^{13}C_{bio}$=3.183-1.051* PO_4^{3-}. The constant 3.~~3~~18 is somewhat higher than estimated for observed $\delta^{13}C$ for which a constant of 2.8 was found by Eide et al. (2017b). This higher constant originates from the over-prediction of the

model ~~of~~ mean $\delta^{13}C$ and PO_4^{3-} at depth, as seen in other models (Sonnerup and Quay, 2012). Eq. (3) assumes a constant biological fractionation as well as a constant $r_{c:p}$ ratio, and these assumptions will introduce some error in the partition of biological and air-sea gas exchange signatures derived from observed $\delta^{13}C$ to PO_4^{3-} ratios (e.g., Eide et al. 2017b). For the purpose of determining $\delta^{13}C_{bio}$ in our model, these assumptions are unproblematic, since $r_{c:p}$ and ε_{photo} actually are taken to be constant in the model formulation. The air-sea gas signature $\delta^{13}C_{AS}$ is approximated as the residual ($\delta^{13}C_{AS} = \delta^{13}C_{model} - \delta^{13}C_{bio}$). $\delta^{13}C_{AS}$ is 0 ‰ when $\delta^{13}C_{model}=\delta^{13}C_{bio}$, i.e. when the $\delta^{13}C$ can be explained by biology only. We express $\delta^{13}C_{bio}$ as a percentage t~~T~~o aid interpretation of the results~~, we express $\delta^{13}C_{bio}$ as a percentage~~ (denoted as $\delta^{13}C_{bio}^{perc}$), because~~ because t the ~~absolute~~ values of $\delta^{13}C_{bio}$ in ‰ ~~in ‰~~ depend strongly on the chosen 'reference' values, i.e. mean DIC, PO_4^{3-}, and $\delta^{13}C$ (compare Schmittner et al., 2013; Sonnerup and Quay, 2012; Broecker and Maier-Reimer, 1992; Lynch-Stieglitz et al., 1995; Eide et al., 2017b). The conversion from $\delta^{13}C_{bio}$ to a percentage is calculated as follows:

$$\delta^{13}C_{bio}^{perc}[\%] = \frac{|\delta^{13}C_{bio}|}{|\delta^{13}C_{bio}|+|\delta^{13}C_{AS}|} * 100\ \% \quad (4)$$

In our analysis, we define the total amount of air-sea carbon exchange as $F_{u+d}=|F_{up}|+|F_{down}|$, with F_{up} as the upward annual carbon flux from the ocean into the atmosphere and F_{down} its downward counterpart (SI 1B and Heinze et al. (1999)). F_{u+d} is relevant for understanding the sensitivity of $\delta^{13}C$. The net carbon exchange is defined as $F_{net}=F_{up}+F_{down}$. The sign of F_{net} indicates whether a region is a source or a sink for carbon and is relevant for understanding changes in pCO_2^{atm}.

3 Results and discussion

3.1 Model control run

The model reproduces the main features of observed marine $\delta^{13}C$, as shown in Fig. 1 and Fig. S2. The modelled global mean surface ocean $\delta^{13}C_{surface}$ of DIC is higher (1.~~96~~88 ‰) than deep ocean $\delta^{13}C_{deep}$ (0.~~7~~67 ‰), creating a mean ocean $\Delta\delta^{13}C$ of 1.21~~0~~ ‰. In the North Atlantic and SO, $\Delta\delta^{13}C$ is least pronounced (0.9 and 0.8 ‰ respectively) due to vertical mixing between surface and deep water during deep water formation and upwelling (Duplessy et al., 1988). $\Delta\delta^{13}C$ increases with water mass age as expected from the increased imprint of remineralisation on $\delta^{13}C$. The mean modelled ocean $\delta^{13}C$ is higher by 0.16~~2~~ ‰ relative to observations (Eide et al., 2017b), which is especially pronounced in the oldest water masses (Fig. S2). This is observed in other models as well and attributed to the model's relative contribution of deep water production in the North Atlantic and Southern Ocean (Sonnerup and Quay, 2012). The modelled global export POC production is 9.6 Gt C yr^{-1} of which 18 % is produced in the SO, which is within the uncertainty of observational estimates (MacCready and Quay, 2001; Nevison et al., 2012; Dunne et al., 2007; Lutz et al., 2007; Schlitzer, 2002). The ~~free~~ atmosphere has a modelled equilibrium pCO_2^{atm} of 279 ppm and a $\delta^{13}C^{atm}$ of -6.50~~44~~ ‰, which developed in the model from the 'best-fit' weathering value F_{eq}^{w} as described above in Sect. 2. Net air-sea gas exchange is close to zero (ventilating ~2~~5~~$\times 10^{-76}$ ~~Pg~~Gt of carbon to the atmosphere

annually)~~, indicating that the model is in equilibrium~~. The resulting drift of the model control over 2000 years is ~~±~~7×10^{-7}~~3~~ ‰ ~~for~~ both $\delta^{13}C^{atm}$ ~~and mean marine $\delta^{13}C$~~, and ~~±~~2~~±5~~×10^{-4}~~3~~ ppm for pCO_2^{atm}.

3.2 Air-sea gas exchange versus biology

The contribution of biology based on equations (2) and (3) to the $\delta^{13}C$ distribution is presented in Fig. 2, broadly in agreement with previous studies (Kroopnick, 1985; Schmittner et al., 2013). The contribution of biology to the modelled $\delta^{13}C$ distribution is generally below 45 % and has a steep gradient from the surface to the deep ocean. The (thermodynamic) fractionation effect of air-sea gas exchange on $\delta^{13}C$ is strongly impeded by the long equilibration time of ^{13}C, which ~~results in~~leaves room for biological processes to contribute significantly to $\delta^{13}C$ and $\Delta\delta^{13}C$ (Eide et al., 2017a; Lynch-Stieglitz et al., 1995; Murnane and Sarmiento, 2000; Schmittner et al., 2013). In the ocean below 250m, the influence of biology increases to 35-45 % due to the remineralisation of POC, with the exception of the Arctic Ocean where no POC production is modelled due to the sea ice cover (Fig. 2b and Fig. S1). $\delta^{13}C_{bio}^{perc}$ is close to 50 % around 1000 m depth in the northern Pacific and Indian oceans, due to the old water masses located there, which have accumulated a large fraction of remineralised DIC. At the surface, air-sea gas exchange dominates the $\delta^{13}C$ signature of DIC as visible from the low $\delta^{13}C_{bio}^{perc}$ (Fig. 2a). The only exception at the surface is in upwelling regions, where a relatively high $\delta^{13}C_{bio}^{perc}$ is expected due to high POC production and upwelled remineralised carbon. High $\delta^{13}C_{bio}^{perc}$ generally corresponds to a low-$\delta^{13}C$ water mass (compare Fig. 1 and Fig. 2), as expected from the upwelling of ^{13}C-depleted DIC and modelled and observed close to the Antarctic continent (Fig. 1a and observations by Eide et al. (2017a)). The results presented in Fig. 2 appear to be quite robust as $\delta^{13}C_{bio}^{perc}$ typically does not change by more than 5-10 % for the wide range of biogeochemical states as explored in the sensitivity experiments presented below.

3.3 Sensitivity of $\Delta\delta^{13}C$ and $\delta^{13}C$

3.3.1 Air-sea gas exchange of carbon

Atmospheric and marine carbon isotopic ratios are generally in thermodynamic disequilibrium due to their relatively long equilibration timescales as compared to the time of contact of a water parcel with the atmosphere ~~because ^{13}C equilibrates ~200 times slower than inert gases like O_2.~~ ~~This difference in equilibration time is due to the fact that DIC~~CO_2 equilibration through the air-sea interface takes ~4 months (Jones et al., 2014) and is inversely related to the Revelle Buffer factor, and slowed down by a factor ~20 as compared to inert gases due to ~~needs to speciate into all marine~~ carbon speciation (i.e. the adjustment of the bicarbonate pool). Again~~species to reach equilibrium (~20x slower than O_2), after which~~ ~10 times slower than CO_2, the air-sea equilibration of the atmospheric isotope ratio $^{13}CO_2/^{12}CO_2$ (i.e. $\delta^{13}C^{atm}$) with marine $DI^{13}C/DI^{12}C$ (i.e. $\delta^{13}C$) takes ~4 years (Jones et al., 2014). The equilibration timescale of the carbon isotopes ~~needs to go through full isotopic exchange between all carbon species to reach equilibrium~~is namely not facilitated by the buffering reaction of CO_2 with H_2O, but instead depends on the DIC:CO_2 ratio of seawater ~~((~~Jones et al., 2014; ~~~10x slower than ^{12}C) (Jones et al., 2014;~~ Galbraith et al., 2015; Broecker and Peng, 1974). Over 90 % of ~~T~~the surface ocean $\delta^{13}C$ signature is ~~dominated~~ set by air-sea gas

exchange outside of upwelling regions across the world's ~~in most ocean regions~~ oceans (Fig. 2), making the equilibration across the air-sea interface important for surface ocean $\delta^{13}C$. Understanding the effects of equilibration across the air-sea interface is thus key to understanding global surface ocean $\delta^{13}C$ signatures. Here we explore two extreme cases, very slow but non-zero gas exchange ('Gas slow', gas exchange rate divided by 4) and very fast gas exchange to bring the air-sea equilibration close to equilibrium ('Gas fast', gas exchange rate multiplied by 4).

~~Any change in the gas exchange rate can thus potentially have a large effect on surface ocean $\delta^{13}C$, depending on~~Our results show that ~~-~~the effects of changes in air-sea gas exchange on $\delta^{13}C$ mainly depend on the prior disequilibrium $\delta^{13}C_{diseq}$ ($\delta^{13}C_{diseq} = \delta^{13}C - \delta^{13}C_{eq}$, where $\delta^{13}C_{eq}$ represents the $\delta^{13}C$ value a water parcel would have had if it would have fully equilibrated with the atmosphere, see also Gruber et al. (1999)). Full ~~I~~isotopic equilibrium with the atmosphere ~~would~~ results in a $\delta^{13}C_{surface}$ of ~0.5 (low latitudes) to ~4 (high latitudes) ‰ (Menviel et al., 2015), where the range is caused by the temperature dependent fractionation (Mook et al., 1986; Zhang et al., 1995). In this study, modelled ε is between 7.7 and 11 ‰. This thermodynamic effect increases the difference between $\delta^{13}C_{surface}$ and $\delta^{13}C_{eq}$ at the poles (Menviel et al., 2015), thus increasing the potential of high latitude surface water to be affected by air-sea gas exchange fluxes.~~approximately 2 ‰ (Murnane and Sarmiento, 2000), since $\delta^{13}C^{atm}$ is about -6.5 ‰ and air-sea fractionation about 8.5 ‰ (Mook et al., 1986).~~

Our gas exchange experiments (Table 1) ~~result~~ show~~in~~ a transient ~~change~~ phase where~~in~~ the net global air-sea gas exchange flux F_{net} is non-zero, which affects pCO_2~~occurs~~ ^{atm} until a new quasi-equilibrium is established (Fig. S3). We find an increase of pCO_2^{atm} by 10~~9~~ ppm (slow~~fast~~ gas exchange) and a decrease by 4 ppm (fast~~slow~~ gas exchange) after 2000 years, respectively. If gas exchange is only changed in the SO (i.e. for 22 % of the global ice-free ocean area), an effect of 3.7 and -0.7~~5~~ ppm ~~and 1 ppm increase~~ is found after 2000 years (Table 2). Gas exchange in the SO can thus cause a disproportionate response (~30 % of the sensitivity) in pCO_2^{atm}. These changes occur in the first ~600 years of the sensitivity experiments (Fig. S3), with the strongest changes occurring after ~100 years. The air-sea pCO_2 difference is smaller at increased gas exchange rates and larger at reduced gas exchange rates (Fig. S4). ~~The spatially variable prior pCO_2 disequilibrium in the SO (Fig. S3) plays an important role in the pCO_2^{atm} sensitivity: The larger increase of the outgassing flux F_{up} of the SO as compared to the carbon uptake flux F_{down} leads to a reduced SO carbon sink and higher pCO_2^{atm} at increased gas exchange rates. The reduction in air-sea C flux for the slow gas exchange experiment causes F_{net} to decrease during the transient phase (Fig. S4 and 5), leading to an increase in pCO_2^{atm} which develops during the first ~600 years. F_{net} is reduced during the transient phase because the slow gas exchange rate decreases Southern Hemispheric net C uptake, while maintaining Northern Hemispheric net C outgassing, also for the global experiment. Interestingly, the $\delta^{13}C^{atm}$ gets decoupled from the pCO_2^{atm} signal as~~ $\delta^{13}C^{atm}$ decreases by 0.3~~(to -6.8 ‰)~~ during fast gas exchange and increases by 0.2 ~~(to -6.3 ‰)~~ when the gas exchange rate is reduced. This is explained by the increase in the global amount of air-sea gas exchange F_{u+d} in the fast gas exchange experiment (4 times more, at 542 Gt C yr^{-1}). Such an increase leads to a smaller thermodynamic disequilibrium, which increases the mean marine $\delta^{13}C$ and lowers $\delta^{13}C^{atm}$. Slow gas exchange reduces F_{u+d} (by 73 % to 36 Gt C yr^{-1}), thus decreasing the role of air-sea gas exchange on surface ocean $\delta^{13}C$. This results in an increased contrast between atmospheric and surface ocean $\delta^{13}C$~~causing less fractionation to occur, -~~which explains the increase of $\delta^{13}C^{atm}$. Moreover, our SO-only experiments show that these effects on $\delta^{13}C^{atm}$ are more

pronounced if gas exchange only changes in the SO. This indicates that the remainder of the ocean offsets part of the atmospheric sensitivity to SO change.

$\delta^{13}C$ shows a different response in high latitudes as compared to the lower latitudes in the surface ocean (Fig. 3a and S5~~6~~): An increased air-sea gas exchange rate lowers the surface ocean $\delta^{13}C$ of DIC by ~~-~~0.2 to ~~-~~0.9 ‰ at the lower latitudes and increases surface ocean $\delta^{13}C$ at high latitudes by 0.2-0.5 ‰ (Fig. 3 and 4). The direction of the response~~se results~~ indicates whether $\delta^{13}C_{diseq}$ is positive or negative, ~~since $\delta^{13}C$ is closer to equilibrium at high gas exchange rates.~~ and is ~~I~~ in line with previous studies (Schmittner et al., 2013; Galbraith et al., 2015) that show that the disequilibrium is negative ($\delta^{13}C < \delta^{13}C_{eq}$) at high latitudes and in low latitude upwelling regions, and positive elsewhere. The sign of $\delta^{13}C_{diseq}$, and thus the direction of the $\delta^{13}C$ response, ~~is is~~can be understood from the difference between the natural $\delta^{13}C$ distribution (Fig. 1) and the ~~potential ~2 ‰~~ $\delta^{13}C_{eq}$ which depends on thermodynamic fractionation (Sect. 2). At increased gas exchange rates (i.e. closer to equilibrium), ~~which would require an~~ $\delta^{13}C$ has to increase~~e in $\delta^{13}C$~~ in cool high latitude surface waters and ~~a~~ has to decrease~~s~~ in warm low latitude surface waters in order to get closer to equilibrium (Menviel et al., 2015; Murnane and Sarmiento, 2000). The net effect of a slower gas exchange rate on surface ocean $\delta^{13}C$ is less pronounced than the effect of an increased gas exchange rate (Fig. S5~~6~~, Fig. 3). The smaller effects seen for slow gas exchange indicate that the control model ocean is a 'slow ocean', i.e. closer to (very) slow gas exchange than to thermodynamic equilibrium (infinitely fast gas exchange).

The effect of the gas exchange rate on marine $\delta^{13}C$ is mostly established in the top 250 to 1000 m of the water column (Fig. 3c, d, Fig. 4). Recording this air-sea gas exchange signal thus strongly depends on the reliability of planktic $\delta^{13}C$-based $\delta^{13}C_{surface}$ reconstructions and knowledge of the living depth represented by the planktic foraminifera. The signal penetrates deepest (to ~2000 m depth) into the North Atlantic (Fig. 4~~, Fig. S7~~), where $\delta^{13}C$ is strongly influenced by air-sea gas exchange (Fig. 2a). However, the interpretation of variations in North Atlantic benthic $\delta^{13}C$ as coming partly from air-sea gas exchange (Lear et al., 2016) is not supported by our experiment. Due to the limited export of the $\delta^{13}C$ signal to depth, the sensitivity of $\Delta\delta^{13}C$ to the gas exchange rate mainly comes from surface ocean $\delta^{13}C$. Globally, the $\Delta\delta^{13}C$ weakens to 0.87~~4~~ ‰ when the thermodynamic disequilibrium is decreased (i.e. 'Gas fast', Fig. 5~~5~~) and $\Delta\delta^{13}C$ strengthens to 1.32 ‰ when the thermodynamic disequilibrium is increased ('Gas slow', Fig. 5). The extent to which thermodynamic equilibrium can develop is thus an efficient way to change the biologically-induced $\Delta\delta^{13}C$ (Murnane and Sarmiento, 2000), however this is only true in lower latitudes where $\delta^{13}C_{diseq}$ is positive:~~.~~ T~~T~~he direction of the high-latitude SO $\Delta\delta^{13}C$ ~~signal~~ sensitivity mirrors~~has an opposite sign~~ the sensitivity of the low latitude regions (Fig. 4) as well as the global mean due to its negative $\delta^{13}C_{diseq}$ ~~and low latitude regions.: When the thermodynamic disequilibrium is decreases (increases), basin-mean $\Delta\delta^{13}C$ in the SO increases (decreases) and thus intensifies the biologically-induced $\Delta\delta^{13}C$ changes (Fig. 4).~~

3.3.2 The biological pump: POC sinking rate

The net effect of a regionally changed biological pump efficiency depends on the sequestration efficiency, which depends on the interplay between the biological pump and ocean circulation (DeVries et al., 2012). A more efficient biological pump (here, a higher POC sinking rate) leads to a loss of carbon to the sediments, which affects pCO_2^{atm} and $\delta^{13}C^{atm}$ on millennial

timescales. Here we present results from a 2000-year simulation (as for the other experiments), which ~~is~~ are thus~~still in a~~ transient ~~phase~~results. ~~To reach a~~A full equilibrium of the system could take as long as 200 000 years (Roth et al., 2014). On these long timescales other processes and feedbacks would occur (Tschumi et al., 2011), which complicates the attribution of changes to a primary trigger. A fast POC sinking rate leads to a pCO_2^{atm} decrease of 2~~3~~8 ppm and higher (~~+~~-0~~6~~.2 ‰) atmospheric $\delta^{13}C$ after 2000 years (Table 2, Fig. S3~~5~~) as well as an ~~shift~~ increase of ~~the~~ mean ocean $\delta^{13}C$ ~~by~~ of ~~~~0.15~~5~~ ‰, caused by the transient sediment burial of low-$\delta^{13}C$ POC. The transient imbalance between weathering and burial fluxes can thus cause profound changes in both marine and atmospheric $\delta^{13}C$, and moreover provides an important feedback for the long-term marine carbon cycle (Roth et al., 2014; Tschumi et al., 2011). In our experiment, an efficient biological pump leads to a global ~~10~~6 % decrease in the amount of air-sea gas exchange F_{u+d} because of efficient export of carbon to depth, thereby lowering the net upward advection of carbon. A mirrored but weaker response is modelled for a decrease in biological pump efficiency: Halving the POC sinking rate leads to a 13 ppm increase in pCO_2^{atm} (of which 2~~3~~8 % can be explained by the SO) and a more negative atmospheric $\delta^{13}C$ (-6.7 ‰) and 7 % increased F_{u+d} (Table 2, Fig. S3~~5~~).

Surface ocean $\delta^{13}C$ is mostly influenced by the changes in productivity and the vertical displacement of the POC remineralisation depth. The deepening of the remineralisation depth has been extensively discussed in the literature (Boyle, 1988; Keir, 1991; Mulitza et al., 1998; Roth et al., 2014), and likely explains lowered mid-depth glacial $\delta^{13}C$ together with changes in ocean circulation (for example, Toggweiler, 1999). POC sinking removes nutrients and preferentially light ^{12}C carbon from the surface ocean, while exporting them to the deep ocean. If POC sinking rates are high, this increases the mean surface ocean $\delta^{13}C$ (contributing to the $\delta^{13}C^{atm}$ increase) by 0.12 ‰ and lowers mean deep ocean $\delta^{13}C$ by 0.01 ‰ (Fig. 6) ~~–~~ with values corrected for ~~despite~~ the overall 0.15 ‰ increase in marine $\delta^{13}C$ which occurs due to transient imbalance between weathering and sediment burial ~~(Fig. 6)~~. Therefore, even though the absolute export production is globally reduced ~~in all productive regions (~~by ~~-~~26 %~~)~~, the biological pump is more efficient as any new nutrients in the surface ocean will immediately be used and exported. With a ~~lower~~ halving of the POC sinking rate, the remineralisation is ~~more~~ confined closer to the surface ocean (Fig. 4). The net effect is that ~~the~~ surface ocean $\delta^{13}C$ ~~becomes~~ is reduced~~lower~~ (in the mean by 0.21 ‰ – corrected for the mean ocean change of 0.04 ‰) throughout the ocean (Fig. 4), because the fractionation effect during photosynthesis is counteracted by the remineralisation of POC (which would normally have occurred at depth). The SO plays a relatively minor role in the~~se changes~~ sensitivity to the POC experiments (Fig. 6b). Changes in deep ocean $\delta^{13}C$ depend on the water mass age (Fig. 6c)~~.~~: Old water (North Pacific) has a larger remineralisation signal when the biological pump is efficient. Independent of the biological pump efficiency, the relatively young waters of the deep North Atlantic generally adopt about the same $\delta^{13}C$ signal as the surface ocean $\delta^{13}C$, which is set by air-sea gas exchange. This is in agreement with a relatively low $\delta^{13}C_{bio}^{perc}$ estimate for the deep North Atlantic (~30 %).

The sensitivity of $\Delta\delta^{13}C$ to changes in POC sinking rate depends strongly on location (Fig. 4 and 6). In general, the $\Delta\delta^{13}C$ strengthens for an increased biological pump efficiency (Fig. 5), and this effect is stronger with water mass age (Fig. 6c, Fig. 4). The downward shift of the remineralisation depth of low-$\delta^{13}C$ POC drives this increase in $\Delta\delta^{13}C$, a mechanism discussed among others by Boyle (1988) and Mulitza et al. (1998) to understand glacial $\Delta\delta^{13}C$ increase. Our results show that the vertical

displacement of the $\delta^{13}C$ profile is most pronounced in the North and South Pacific ~~for both faster and slower POC sinking rates~~ (Fig. 4~~ and Fig. S7~~). The North Atlantic $\Delta\delta^{13}C$ is much less affected as these waters are mostly influenced by air-sea gas exchange. Instead, the entire North Atlantic profile is shifted more than in the other ocean basins (Fig. 4~~S7~~). $\Delta\delta^{13}C$ weakens for a reduced biological pump efficiency (Fig. 4 and 5), especially in older water where $\delta^{13}C_{bio}^{perc}$ is higher (Fig. 2a). It is worth noting, however, that the changes in $\Delta\delta^{13}C$ in the SO are comparably small because the vertical mixing in the SO of the low-$\delta^{13}C$ deep water mostly causes shifts in the entire $\delta^{13}C$ profile, not a change in the gradient (Fig. 4).

3.3.3 The biological pump: SO nutrient depletion

Consistent with previous studies (Primeau et al., 2013; Marinov et al., 2006; Sarmiento et al., 2004), we find a large atmospheric impact of our SO nutrient depletion experiment. The high SO nutrient uptake efficiency (i.e. an efficient biological pump) causes a ~~51~~44 ppm reduction in pCO_2^{atm} after 2000 years. The V_{max} experiment ~~largely~~ reaches quasi-equilibrium~~ates~~ after ~800 years, as seen from the time evolution of pCO_2^{atm} and $\delta^{13}C^{atm}$ (Fig. S3~~5~~). $\delta^{13}C^{atm}$ increases to -6.1~~0~~ ‰ due to the increased surface ocean $\delta^{13}C$ (Fig. 7a). This 0.4~~5~~ ‰ increase is high compared to the results of Menviel et al. (2015), who found a $\delta^{13}C^{atm}$ sensitivity of 0.1-0.2 ‰ in response to changes in SO nutrient utilization. The different development time as compared to the fast POC sinking rate experiment is explained by the absence of long-term loss of carbon to the sediments in the V_{max} experiment, ~~probably~~ because transport and water-column remineralisation within the SO limits an increase in POC burial there. In the SO, net carbon uptake (F_{net}) increases four~~ive~~fold to 1.5 Gt C yr^{-1} (Fig. S6~~8~~) because the high nutrient and carbon consumption transport carbon~~C~~ into the ocean interior and do not permit CO_2 to escape to the atmosphere ~~from the deep ocean~~.

SO ~~E~~export production of POC is increased ~~in the SO~~ (Fig. S7~~9~~) by a factor 2.4~~5~~, causing global POC export production to increase by 15~~7~~ % albeit reducing lower-latitude productivity (non-SO up to ~35 °N) by 13~~1~~ %. This relocation of global POC export production in response to SO increased nutrient uptake efficiency is in agreement with earlier studies (Primeau et al., 2013; Marinov et al., 2006).

The increased surface ocean $\delta^{13}C$ signature everywhere north of the SO sea ice edge (Fig. 7a) is in the SO attributed to increased POC export production counteracted by a decreased F_{u+d} ~~in the SO~~ (which would reduce $\delta^{13}C_{surface}$ in the SO because of the negative $\delta^{13}C_{diseq}$, Fig. 3 and S5~~6~~). In lower latitudes, the decreased F_{u+d} (which increases $\delta^{13}C_{surface}$ in lower latitudes because of the positive $\delta^{13}C_{diseq}$, Fig. 3 and S5~~6~~) dominates the effect of the 1~~1~~3 % lower POC export production on $\delta^{13}C_{surface}$. At depth and under the sea ice in the Antarctic where deep water upwells, the imprint of additional POC ~~remineralisation~~remineralisation at depth decreases $\delta^{13}C$ of DIC (Fig. 7). This decrease in $\delta^{13}C$ is only visible in water masses downstream of the SO (Fig.7b and c) and most pronounced in the deep North Pacific (Fig. 7c). The increased nutrient uptake rate in the SO ~~strongly~~ increases global mean $\Delta\delta^{13}C$ by 0.4 ‰ (Fig. 5) as well as~~nd~~ increasing $\Delta\delta^{13}C$ in all ocean basins (Fig. 4), as seen for the fast POC sinking rate experiment. ~~As for a changed POC sinking rate,~~ $\Delta\delta^{13}C$ is affected more in older waters, where a more pronounced remineralisation imprint has developed (Fig. 4).

Besides effects on the $\delta^{13}C$ distribution (Fig. 7), the O_2 and PO_4^{3-} distributions change as well: The O_2 distribution is reorganised such that surface ocean O_2 is increased (by up to 210 µmol kg^{-1}, with largest changes in the SO), while deep ocean O_2 is reduced downstream of the SO (by up to 40 µmol kg^{-1}). Surface ocean PO_4^{3-} is reduced mostly in the SO (by up to -0.8 µmol kg^{-1}). This signal is however too small to significantly increase mean deep ocean PO_4^{3-}. This implies a reduction in global preformed phosphate governed by the efficient nutrient uptake in the SO, see also Primeau et al., (2013). SO nutrient drawdown can thus cause negligible mean (deep) ocean PO_4^{3-} and $\delta^{13}C$ changes, despite causing large changes in local $\delta^{13}C$ and $\Delta\delta^{13}C$ through the interplay between biology and air-sea gas exchange. ~~This is i~~Interesting in light of glacial proxy interpretation, ~~as~~ the fit to the ~~deviations from the~~ $\delta^{13}C$:PO_4^{3-} relationship is improved throughout the ocean for the V_{max} experiment, similar to the effects of the 'Gas slow' experiment (~~Sect. 2~~Fig. 8). Changes in the goodness-of-fit of $\delta^{13}C$ and PO_4^{3-} data to the $\delta^{13}C$:PO_4^{3-} relationship (i.e. $\delta^{13}C_{bio}$=3.18-1.05* PO_4^{3-}, Sect. 2) are usually ~~usually~~ interpreted as ~~the influence of~~changes in ventilation or air-sea gas exchange ~~on $\delta^{13}C$~~ (Eide et al., 2017b; Lear et al., 2016). However~~, but~~, here we show that changes in the fit represent the relative importance of biology and air-sea gas exchange in determining $\delta^{13}C$, as both changes in $\delta^{13}C_{diseq}$ (i.e. gas exchange rate experiments) as well as changes in the biological pump can affect the goodness-of-fit to the $\delta^{13}C$:PO_4^{3-} relationship (Fig. 8)~~could thus also come from changes in nutrient uptake efficiency~~.

~~3~~3.3.4 Southern Ocean sea ice cover

The sea ice cover of the SO changes considerably over glacial-interglacial cycles, as well as on seasonal timescales (Crosta (2009) and Fig. A22 therein). In general, the model~~s~~ sea ice cover will inhibit light penetration into the surface ocean and limit~~s well as~~ air-sea gas exchange based on its thickness (Sect. 2). ~~Here~~ In the sensitivity experiments we assume complete inhibition of both light and air-sea carbon exchange by the sea ice. In this section we thus explore the effect of both biological production and air-sea gas exchange in two extreme cases, i) the largest realistic sea ice cover based on the glacial maximum winter extreme (50° S) and ii) the smallest sea ice cover based on the contemporary summer minimum sea ice extent (70° S). Note that there is a constant sea ice cover about north of 70°N and south of 60° S in the control run of the model. Therefore, the strongest marine $\delta^{13}C$ change is expected south of 60° S for a decreased sea ice cover and between 50-60° S for an increased sea ice cover, as this is the area where ice cover is altered relative to the control run. Ocean circulation changes that could result from a changed sea ice cover are not taken into account, as we want to study the potential isolated effect of sea ice on $\delta^{13}C$ through biological and air-sea gas exchange changes.

Both local and global air-sea carbon fluxes are influenced by a change of the SO sea ice cover, which results in changes in pCO_2^{atm} and $\delta^{13}C^{atm}$. In our experiment, pCO_2^{atm} increases by 9~~5~~ ppm for an increased sea ice cover and decreases by 6~~5~~ ppm for a decreased sea ice cover (Table 2, Fig. S3~~5~~). As noted in Sect. 3.3.1, a change in pCO_2^{atm} is governed by a transient change in the net air-sea gas exchange flux F_{net} until a new equilibrium is established. An extended ice cover causes more CO_2 to remain in the atmosphere because the additional ice covers a part of the SO that is a sink for CO_2 ~~in the control run~~ (Fig. S4~~3~~ - Control). As the net global air-sea gas exchange F_{net} approaches equilibrium, the non-SO ocean therefore becomes a smaller source for carbon. This reduces the net gas exchange F_{net} inside and outside of the SO by ~40-50 %~~about one third~~. Our results

show that the effects of a changed sea ice cover on pCO_2^{atm} are yet to be fully understood: Stephens and Keeling (2000) for example modelled a strong decrease of pCO_2^{atm} in response to an increased sea ice cover south of the Antarctic Polar Front, because they mostly cover a part of the SO that is a sesourcse of carbonC to the atmosphere. In our study, the reduction in pCO_2^{atm} by 65 ppm due to a reduced sea ice cover is attributable to the POC production in the earlier previously ice-covered area between ~60° S and 70° S. In a sensitivity experiment where the ice cover influences air-sea gas exchange only, the sea ice retreat leads to an increase in pCO_2^{atm} because the region below the ice is strongly supersaturated in carbonC with respect to the atmosphere. The increased sea ice cover leads to a complete suppression of air-sea gas exchange south of 50° S. Since this region is in negative carbon isotopic disequilibrium with the atmosphere ($\delta^{13}C < \delta^{13}C_{eq}$, Fig. S6), the ice cover inhibits a $\delta^{13}C$ flux into the ocean. As a result, $\delta^{13}C^{atm}$ increases to -6.21 ‰, and while the opposite happens for a reduced sea ice cover, leading to a lowered $\delta^{13}C^{atm}$ (-6.6 ‰).

The increased sea ice cover over the SO results in a surface ocean $\delta^{13}C$ reduction relative to the control of -0.5 ‰ to -0.1 ‰ in the SO (Fig. 4, Fig. 9), while $\delta^{13}C$ is increasesd outside of the SO with by 0-0.2 ‰ (Fig. 98a). The reduction is especially pronounced between 40-60° S. The ~40 % reduced POC export production in the SO due to light inhibition by the sea ice cover causes a major part of the SO surface $\delta^{13}C$ reduction, as the absence of photosynthesis will cause lower surface ocean $\delta^{13}C$. Next to that, the reduced air-sea gas exchange F_{u+d} in the SO also leads to a lowered surface ocean $\delta^{13}C$ signature. About the opposite happens when we simulate a strongly decreased sea ice cover (only ice south of 70° S): A small reduction of $\delta^{13}C$ is modelled outside the SO, but the SO $\delta^{13}C_{surface}$ locally becomes up to ~0.8 ‰ higher relative to the control (Fig. 98b) as the increased amount of air-sea gas exchange F_{u+d} decreases the carbon isotopic disequilibrium and increases POC production in the newly exposed area, both acting to increase $\delta^{13}C$ of DIC.

The effect of a changed ice cover on deep ocean $\delta^{13}C$ is less than ~0.1 ‰ (Fig. 98c, d) as the surface signal is diluted while it follows the general ocean circulation. As for air-sea gas exchange (Sect. 3.3.1), no pronounced deep ocean $\delta^{13}C$ signal is found outside of the SO due to sea ice cover changes (this opposed to interpretations by Lear et al., 2016). Global mean $\Delta\delta^{13}C$ is not significantly affected by changes in the SO sea ice cover (Fig. 5) because the low and high latitude effects on $\delta^{13}C_{surface}$ cancel each other out. The SO $\Delta\delta^{13}C$ however weakens considerably to 0.4 ‰ when the 50-60° S region becomes covered with sea ice and strengthens to 1 ‰ if the sea ice is removed between 60-70° S (Fig. 4S10). The presence or absence of a sea ice cover should thus be clearly visible in especially planktic SO $\delta^{13}C$ sediment records. The effects on $\Delta\delta^{13}C$ advance spreads downstream of the SO, where $\Delta\delta^{13}C$ is increased by up to 0.2 ‰ throughout in the Pacific and Indian oceanOceans for an increased SO sea ice cover (Fig. 4S10)).

3.4 Modelled versus observed $\Delta\delta^{13}C$ variations

The variations in $\Delta\delta^{13}C$ on glacial-interglacial timescales provide researchers with a tracer to study the biogeochemical state of the past global ocean, under the condition that we can interpret (variations in) $\Delta\delta^{13}C$. The idealised perturbations made to the (Southern) Ocean in this study show that global mean $\Delta\delta^{13}C$ is particularly sensitive to an increased gas exchange rate and changes in the efficiency of the biological pump. Global mean $\Delta\delta^{13}C$ varies by up to about ~±0.354 ‰ around the pre-industrial

model reference (1.2 ‰) in response to biogeochemical change (Fig. 5) - under the assumption of a constant ocean circulation. However, the sensitivity of $\Delta\delta^{13}C$ to biogeochemical changes depends strongly on location for all sensitivity experiments (Fig. 4), possibly explaining part of the incoherency of reconstructed planktic and benthic foraminiferal $\delta^{13}C$ from sediment cores (Oliver et al., 2010). In general, such $\Delta\delta^{13}C$ reconstructions show $\Delta\delta^{13}C$ variations of ~1 ‰ over the past 350 000 years (Boyle, 1988; Shackleton et al., 1983; Shackleton and Pisias, 1985; Ziegler et al., 2013; Charles et al., 2010; Oliver et al., 2010). Ocean circulation changes explain at least part of these variations in $\Delta\delta^{13}C$ (Charles et al., 2010; Heinze et al., 1991; Jansen, 2017; Heinze and Hasselmann, 1993; Oppo et al., 1990; Toggweiler 1999). However, the changes in the biogeochemical state of the ocean imposed in our experiments show that variations in $\Delta\delta^{13}C$ could be strongly influenced by (SO) biogeochemistry as well. $\Delta\delta^{13}C$ is increased during glacials and reduced during interglacials across a large set of sediment cores (Boyle, 1988; Charles et al., 2010; Oliver et al., 2010; Ziegler et al., 2013). Rapid and large changes have been documented for SO $\Delta\delta^{13}C$ records (Ziegler et al., 2013), and here we show that biogeochemical changes in the SO affect $\Delta\delta^{13}C$ globally. Our results show that an increase in mean $\Delta\delta^{13}C$ could biogeochemically result from slower gas exchange, increased POC sinking rates, or an increased nutrient uptake rate in the SO (Fig. 4 and 5). Such biogeochemical changes have been associated with glacial periods (for example, Ziegler et al. (2013)), and are potential candidates to explain part of the $\Delta\delta^{13}C$ increase in interplay with stronger ocean stratification. Sediment-core reconstructions of $\Delta\delta^{13}C$ show that an increased $\Delta\delta^{13}C$ can originate from a downward shift of the metabolic imprint of low-$\delta^{13}C$ POC which would increase shallow $\delta^{13}C$ (Boyle, 1988; Charles et al., 2010; Mulitza et al., 1998; Toggweiler, 1999), and/or a deep ocean $\delta^{13}C$ decrease (Broecker, 1982; Boyle, 1988; Oliver et al., 2010) with little variation recorded for surface ocean $\delta^{13}C$. The absence of a clear surface $\delta^{13}C$ signal could in the SO be the net effect of an increased sea ice cover (locally decreasing $\delta^{13}C$, Fig. 4 and 9~~8~~a) and an increased biological pump efficiency (locally increasing $\delta^{13}C_{surface}$, Fig. 6a and b, Fig. 7a) or increased SO thermodynamic equilibrium (Fig. 3a and b) – if these opposing signals get mixed. A pronounced deep ocean $\delta^{13}C$ decrease is associated with an efficient biological pump and older water masses in our study (Fig. 4). Interestingly, large local changes in deep ocean $\delta^{13}C$ and $\Delta\delta^{13}C$ do not necessarily imply changes in mean deep ocean PO_4^{3-} (Sect. 3.3.3). ~~The absence of a pronounced PO_4^{3-} change despite $\Delta\delta^{13}C$ changes shows that changed ocean circulation (Toggweiler, 1999) is not the only candidate for explaining the reconstructed deepening of low-$\delta^{13}C$ water and small deep-ocean glacial-interglacial PO_4^{3-} variation.~~

The local character of the $\Delta\delta^{13}C$ sensitivity (Fig. 4) implies that correlations between sediment core $\Delta\delta^{13}C/\delta^{13}C$ variations and global parameters (e.g. pCO_2) are not easily extrapolated to other sediment cores over large distances. Analysis of SO $\Delta\delta^{13}C$ reconstructions from sediment cores at 42° S and 46° S (Charles et al., 2010) for example shows that there is a strong correlation between these cores and Northern Hemisphere climate fluctuations. We expect that this strong correlation does not exist for cores further south in the SO because our results indicate that the SO south of ~50-60° S often has a different $\Delta\delta^{13}C$ response to biogeochemical change than the rest of the ocean.

Interglacial periods are generally thought to be associated with a decrease in the efficiency of the biological pump and increased deep-ocean ventilation via southern-sourced water masses (Gottschalk et al., 2016). Increased deep-ocean ventilation might be driven by increased winds (Tschumi et al., 2011), which would (apart from changing the SO circulation pattern) also

increase gas exchange rates. Each of these processes indeed reduces $\Delta\delta^{13}C$ in the mean in our experiments (Fig. 5), although less pronounced so in the SO (Fig. 4 ~~and Fig. S7~~). However, the interglacial reduction of $\Delta\delta^{13}C$ seems to originate from a deep ocean $\delta^{13}C$ increase as compared to the glacial deep ocean $\delta^{13}C$ (Broecker, 1982; Charles et al., 2010; Oliver et al., 2010). Our results show that neither an inefficient biological pump nor fast gas exchange can be associated with a pronounced deep sea $\delta^{13}C$ increase relative to our control, because~~as~~ their effects are restricted to the surface ocean. On the other hand, the interglacial decrease of $\Delta\delta^{13}C$ is a decrease as compared to the glacial state: If glacial SO nutrient uptake was higher (V_{max}), a return to the 'normal' state (i.e. the model control run) would result in a major decrease of $\Delta\delta^{13}C$ (Fig. 4 and 5).

3.5 The relationship between $\Delta\delta^{13}C$, $\delta^{13}C^{atm}$ and pCO_2^{atm}

One would expect variations of $\delta^{13}C^{atm}$ as well as $\Delta\delta^{13}C$ to correlate with variations in pCO_2^{atm}, because similar processes (biology and air-sea gas exchange) steer their distribution/concentrations (Shackleton and Pisias, 1985; this article). $\Delta\delta^{13}C$ is considered a promising proxy for reconstructions of pCO_2^{atm} for times predating ice-core records (Lisiecki, 2010). Here we show that a positive linear relationship between $\delta^{13}C^{atm}$ and global mean $\Delta\delta^{13}C$ (Fig. 109a) ~~and a negative linear relationship between pCO_2^{atm} and global mean $\Delta\delta^{13}C$ (Fig. 9b)~~ holds over a wide range of biogeochemical states as simulated in the sensitivity experiments. However, the negative linear relationship between pCO_2^{atm} and global mean $\Delta\delta^{13}C$ (Fig. 10b) is weak (R^2=0.39). However, ~~This result supports~~ previous studies do ~~that~~ show ~~both~~ the existence of a ~~local~~ correlation between local $\Delta\delta^{13}C$ and pCO_2^{atm} (such as found by for example Dickson et al. (2008)), and correlation of modified $\Delta\delta^{13}C$ between ocean basins with pCO_2^{atm} (Lisiecki, 2010). The effects of ocean circulation on glacial-interglacial $\delta^{13}C^{atm}$ changes, not studied here, are most pronounced in response to Antarctic Bottom Water formation rate variations and are of the order of 0-0.15 ‰ (Menviel et al., 2015). Our results show that $\delta^{13}C^{atm}$ varies by up to about ~~~~±0.5 ‰ in response to biogeochemical changes (Table 2). ~~Figure 9a shows that c~~Changes in the POC sinking rate lie approximately along a line in $\delta^{13}C^{atm}$:$\Delta\delta^{13}C$ space (Fig. 10a), suggesting that changes in the biological pump efficiency ~~is~~ are important for the $\delta^{13}C^{atm}$:$\Delta\delta^{13}C$ relationship. Likewise, both the gas exchange rate and ~~relationship~~ biological pump experiments lie along an approximate lines in~~between~~ pCO_2^{atm}~~:~~ ~~and~~ $\Delta\delta^{13}C$ space (Fig. 10b, albeit a different one - leading to a low total correlation). ~~is mostly coming from the biological pump, as air-sea gas exchange affects $\Delta\delta^{13}C$ much more than pCO_2^{atm} (Fig. 9b).~~ Changes in air-sea gas exchange (as simulated in the gas exchange and sea ice cover experiments) affect $\delta^{13}C^{atm}$ more than $\Delta\delta^{13}C$. This confirms the idea that $\Delta\delta^{13}C$ is governed by biological processes and will also set $\delta^{13}C^{atm}$, unless air-sea gas exchange gets the chance to dominate $\delta^{13}C^{atm}$. The high potential of SO air-sea gas exchange to ~~steer~~ change $\delta^{13}C^{atm}$ (Table 2: Sea ice and gas exchange rate experiments) complements recent studies showing that increased SO ventilation of deep ocean carbon is a likely candidate for glacial-interglacial $\delta^{13}C^{atm}$ excursions – which are of the order of 0.5 ‰ (Bauska et al., 2016; Eggleston et al., 2016; Lourantou et al., 2010; Menviel et al., 2015).

4 Summary and conclusions

This study addresses the sensitivity of modelled marine and atmospheric $\delta^{13}C$ and $\Delta\delta^{13}C$ to changes in ~~the~~ biogeochemical parameters under constant ocean circulation, focusing on the contribution of the SO (the ocean south of 45° S, 22 % of the global ice-free ocean area). Variations of $\Delta\delta^{13}C$ recorded in sediment records are sensitive to ocean circulation changes as shown in previous studies, but here we show that the biogeochemical state of the (Southern) Ocean also can have large effects on $\Delta\delta^{13}C$ across all ocean basins. Using the ocean biogeochemistry general circulation model HAMOCC2s, a set of sensitivity experiments was carried out, which focuses on the biogeochemical aspects known to be important for $\delta^{13}C$ and $\Delta\delta^{13}C$. Specifically, the experiments explore changes in air-sea gas exchange rate, sea ice extent (influencing both biological production and the air-sea gas exchange of carbon) and the efficiency of the biological pump through the POC sinking rate and nutrient uptake rate.

The results show the important role of the SO in determining global $\delta^{13}C$ and $\Delta\delta^{13}C$ sensitivities, as well as the strong spatial differences in these. A new quasi-equilibrium state developed mostly within the first 100-800 years of the sensitivity experiments, except for the POC sinking experiment where an imbalance between weathering and burial causes a long-term drift. The $\delta^{13}C$ signature is governed by different processes depending on location: Air-sea gas exchange sets surface ocean $\delta^{13}C$ in all ocean basins, contributing 60-100 % to the $\delta^{13}C$ signature. At depth and with increasing water mass age, the influence of biology increases to 50 % in the oldest water masses (North Pacific) due to POC remineralisation. This spatial pattern behind the $\delta^{13}C$ signature of a water parcel results in a non-uniform sensitivity of $\delta^{13}C$ to biogeochemical change. Global mean $\Delta\delta^{13}C$ varies by up to ~~~~about ±0.354 ‰ due to biogeochemical state changes in our experiments (at a constant ocean circulation) (Fig. 5). This amplitude is almost half of the reconstructed variation in $\Delta\delta^{13}C$ on glacial-interglacial timescales (1 ‰), and could thus contribute to variations in $\Delta\delta^{13}C$ together with ocean circulation changes. However, $\Delta\delta^{13}C$ can have a different response on a basin scale: The ocean's oldest water (North Pacific) responds most to biological changes, the young deep water (North Atlantic) responds strongly to air-sea gas exchange changes, and the vertically well-mixed water (SO) has a low or even reversed $\Delta\delta^{13}C$ sensitivity as compared to the other basins. The amplitude of the $\Delta\delta^{13}C$ sensitivity can be higher at decreasing scale, as seen from a maximum sensitivity of about ~~-0.6 ‰ on ocean basin scale (Fig. 4). Interestingly, the direction of both glacial (intensification of $\Delta\delta^{13}C$) and interglacial (weakening of $\Delta\delta^{13}C$) $\Delta\delta^{13}C$ change matches changes in biogeochemical processes thought to be associated with these periods. This supports the idea that biogeochemistry explains part of the reconstructed variations in $\Delta\delta^{13}C$, in addition to changes in ocean circulation.

An increased gas exchange rate has the potential to reduce the biologically-induced $\Delta\delta^{13}C$ through the reduction of surface ocean and atmospheric $\delta^{13}C$. Increased gas exchange however only reduces $\Delta\delta^{13}C$ in the low latitudes: In high latitudes, increased gas exchange will increase $\Delta\delta^{13}C$ (by increasing $\delta^{13}C_{surface}$) because of the negative disequilibrium $\delta^{13}C_{diseq}$ (i.e. $\delta^{13}C < \delta^{13}C_{eq}$) in this region, and thus a potential to increase $\delta^{13}C_{surface}$ (section 3.3.1). Notably, pCO_2^{atm}, $\delta^{13}C^{atm}$ and marine $\delta^{13}C$ are shown to be disproportionally sensitive to SO gas exchange rate changes~~: The SO only experiment results in a pCO_2^{atm} and mean $\Delta\delta^{13}C$ change as high as ~50 % of the Global experiment (for 'Gas fast')~~.

Changes in the efficiency of the biological pump also have a major potential to alter $\Delta\delta^{13}C$ as well as pCO_2^{atm} and $\delta^{13}C^{atm}$. The globally increased POC sinking rate experiment shows that $\Delta\delta^{13}C$ strengthens in low latitudes (and more so in older waters) by deepening the low-$\delta^{13}C$ signature of remineralised POC, while SO $\Delta\delta^{13}C$ is not very sensitive to POC sinking rates. The SO effects are comparably small because the vertical mixing in the SO of the low-$\delta^{13}C$ deep water only causes shifts in the entire $\delta^{13}C$ profile, not a change in the gradient (Fig. 4). Increased POC sinking causes a long-term imbalance between weathering and sediment burial which leads to an increase in mean $\delta^{13}C$ and $\delta^{13}C^{atm}$ (of about ~~+~~0.15~~2~~ ‰) after 2000 years. Increased nutrient uptake in the SO (V_{max} experiment) results in 13 % lower ~~a~~ non-SO POC export production up to ~35 °N~~, ~11 % lower POC export production outside of the SO,~~ in agreement with previous studies on the role of the SO biological pump in lower latitude productivity. Interestingly, the increase of $\Delta\delta^{13}C$ in all ocean basins occurs without significantly changing mean (deep) ocean PO_4^{3-}, which advocates for increased SO nutrient uptake to explain (part of) glacial-interglacial $\Delta\delta^{13}C$ variations.~~.~~ Furthermore, our results show that improved goodness-of-fit of the model data to the $\delta^{13}C$:PO_4^{3-} relationship can be driven by reduced gas exchange as well as biological uptake efficiency in the SO, since both increase the importance of biology relative to air-sea gas exchange for $\delta^{13}C$. Caution should thus be exercised when interpreting changes in the fit of observations to the $\delta^{13}C$:PO_4^{3-} relationship as changes in ocean ventilation or air-sea gas exchange alone.

A significant linear relationship was found across the sensitivity experiments between ~~pCO_2^{atm} and $\Delta\delta^{13}C$ as well as~~ $\delta^{13}C^{atm}$ and $\Delta\delta^{13}C$ (R^2=0.71), and a weaker one (R^2=0.39) for pCO_2^{atm} and $\Delta\delta^{13}C$.~~.~~ This result shows that paleo-reconstructions of $\delta^{13}C^{atm}$ ~~pCO_2^{atm}~~ based on $\Delta\delta^{13}C$ could be valid for a wide range of biogeochemical states. Previous studies have shown good correlation between pCO_2^{atm} and local $\Delta\delta^{13}C$, but our results suggest that the relationship may not be valid if both biological and gas exchange rate changes occur. ~~Such a wide applicability of a pCO_2^{atm}:$\Delta\delta^{13}C$ relationship agrees with previous studies that find pCO_2^{atm}:$\Delta\delta^{13}C$ correlation for sediment cores around the globe.~~ The maximum response of $\delta^{13}C^{atm}$ to the biogeochemical changes imposed in our experiments (up to 0.5 ‰) is larger than the idealised maximum effect of ocean circulation changes on $\delta^{13}C^{atm}$ (0-0.15 ‰ (Menviel et al., 2015)), which underlines the potential importance of biogeochemical processes for variations in $\delta^{13}C^{atm}$. The high potential of SO air-sea gas exchange to steer $\delta^{13}C^{atm}$ (Table 2: Sea ice and gas exchange rate experiments) complements recent studies showing that increased SO ventilation of deep ocean carbon is a likely candidate for glacial-interglacial $\delta^{13}C^{atm}$ excursions.

As an outlook, the use of a more complex model with a higher horizontal and vertical resolution and a shorter time-step (resolving seasonal variations) could provide valuable additional information. For example, the role of different regions within the SO on the global $\delta^{13}C$ distribution could be better studied with a more complex model. Sediment core-based reconstructions of the global carbon cycle could possibly be aided by a more complex model with a finer grid and higher time resolution, by providing more detailed information on the contribution of biogeochemical processes to local ocean tracers. Next to that, exploring the effect on $\Delta\delta^{13}C$ of a glacial model circulation field could provide a way to quantify the maximum combined effect of circulation and biogeochemical change on $\Delta\delta^{13}C$.

Acknowledgements. The authors would like to thank two anonymous reviewer for their constructive and helpful comments, which improved this manuscript. This study is a contribution to the project "Earth system modelling of climate variations in the Anthropocene" (EVA; grant no. 229771) as well as the project "Overturning circulation and its implications for global carbon cycle in coupled models" (ORGANIC; grant no. 239965) which are both funded by the Research Council of Norway. This is a contribution to the Bjerknes Centre for Climate Research (Bergen, Norway). Storage resources were provided by the Norwegian storage infrastructure of Sigma2 (NorStore project ns2980k). Anne Morée is grateful for PhD funding through the Faculty for Mathematics and Natural Sciences of the University of Bergen and the Meltzer Foundation. Christoph Heinze acknowledges sabbatical support from the Faculty for Mathematics and Natural Sciences of the University of Bergen.

References

Bauska, T. K., Baggenstos, D., Brook, E. J., Mix, A. C., Marcott, S. A., Petrenko, V. V., Schaefer, H., Severinghaus, J. P., and Lee, J. E.: Carbon isotopes characterize rapid changes in atmospheric carbon dioxide during the last deglaciation, P Natl Acad Sci USA, 113, 3465-3470, 10.1073/pnas.1513868113, 2016.

Boyle, E. A.: The role of vertical chemical fractionation in controlling late Quaternary atmospheric carbon dioxide, Journal of Geophysical Research: Oceans, 93, 15701-15714, 10.1029/JC093iC12p15701, 1988.

Broecker, W. S.: Ocean chemistry during glacial time, Geochimica et Cosmochimica Acta, 46, 1689-1705, https://doi.org/10.1016/0016-7037(82)90110-7, 1982.

Broecker, W. S., and Maier-Reimer, E.: The influence of air and sea exchange on the carbon isotope distribution in the sea, Global Biogeochemical Cycles, 6, 315-320, 10.1029/92GB01672, 1992.

Broecker W, S., and Peng, T. H.: Gas exchange rates between air and sea, Tellus, 26, 21-35, 10.1111/j.2153-3490.1974.tb01948.x, 1974.

Broecker, W. S., and Peng, T.-H.: The role of CaCO3 compensation in the glacial to interglacial atmospheric CO2 change, Global Biogeochemical Cycles, 1, 15-29, 10.1029/GB001i001p00015, 1987.

Broecker, W. S., and McGee, D.: The 13C record for atmospheric CO2: What is it trying to tell us?, Earth and Planetary Science Letters, 368, 175-182, http://dx.doi.org/10.1016/j.epsl.2013.02.029, 2013.

Charles, C. D., Pahnke, K., Zahn, R., Mortyn, P. G., Ninnemann, U., and Hodell, D. A.: Millennial scale evolution of the Southern Ocean chemical divide, Quaternary Science Reviews, 29, 399-409, 10.1016/j.quascirev.2009.09.021, 2010.

Craig, H.: Isotopic standards for carbon and oxygen and correction factors for mass-spectrometric analysis of carbon dioxide, Geochimica et Cosmochimica Acta, 12, 133-149, https://doi.org/10.1016/0016-7037(57)90024-8, 1957.

Crosta, X.: Antarctic Sea Ice History, Late Quaternary, in: Encyclopedia of Paleoclimatology and Ancient Environments, edited by: Gornitz, V., Springer Netherlands, Dordrecht, 31-34, 2009.

Crucifix, M.: Distribution of carbon isotopes in the glacial ocean: A model study, Paleoceanography, 20, n/a-n/a, 10.1029/2005PA001131, 2005.

Curry, W. B., and Oppo, D. W.: Glacial water mass geometry and the distribution of δ13C of ΣCO2 in the western Atlantic Ocean, Paleoceanography, 20, n/a-n/a, 10.1029/2004PA001021, 2005.

DeVries, T., Primeau, F., and Deutsch, C.: The sequestration efficiency of the biological pump, Geophysical Research Letters, 39, L13601, 10.1029/2012GL051963, 2012.

Dickson, A. J., Leng, M. J., and Maslin, M. A.: Mid-depth South Atlantic Ocean circulation and chemical stratification during MIS-10 to 12: implications for atmospheric CO2, Clim. Past, 4, 333-344, 10.5194/cp-4-333-2008, 2008.

Dunne, J. P., Sarmiento, J. L., and Gnanadesikan, A.: A synthesis of global particle export from the surface ocean and cycling through the ocean interior and on the seafloor, Global Biogeochemical Cycles, 21, GB4006, 10.1029/2006GB002907, 2007.

Duplessy, J. C., Shackleton, N. J., Fairbanks, R. G., Labeyrie, L., Oppo, D., and Kallel, N.: Deepwater source variations during the last climatic cycle and their impact on the global deepwater circulation, Paleoceanography, 3, 343-360, 10.1029/PA003i003p00343, 1988.

Eggleston, S., Schmitt, J., Bereiter, B., Schneider, R., and Fischer, H.: Evolution of the stable carbon isotope composition of atmospheric CO2 over the last glacial cycle, Paleoceanography, 31, 434-452, 10.1002/2015PA002874, 2016.

Eide, M., Olsen, A., Ninnemann, U. S., and Eldevik, T.: A global estimate of the full oceanic 13C Suess effect since the preindustrial, Global Biogeochemical Cycles, 31, 492-514, 10.1002/2016GB005472, 2017a.

Eide, M., Olsen, A., Ninnemann, U. S., and Johannessen, T.: A global ocean climatology of preindustrial and modern ocean δ13C, Global Biogeochemical Cycles, 31, 515-534, 10.1002/2016GB005473, 2017b.

Emerson, S., and Hedges, J.: Chemical oceanography and the marine carbon cycle, Cambridge University Press, Cambridge, xi, 453 p. 458 p. of col. plates pp., 2008.

Galbraith, E. D., Kwon, E. Y., Bianchi, D., Hain, M. P., and Sarmiento, J. L.: The impact of atmospheric pCO_2 on carbon isotope ratios of the atmosphere and ocean, Global Biogeochemical Cycles, 29, 307-324, 10.1002/2014GB004929, 2015.

Gottschalk, J., Skinner, L. C., Lippold, J., Vogel, H., Frank, N., Jaccard, S. L., and Waelbroeck, C.: Biological and physical controls in the Southern Ocean on past millennial-scale atmospheric CO2 changes, 7, 11539, 10.1038/ncomms11539 https://www.nature.com/articles/ncomms11539#supplementary-information, 2016.

Gruber, N., Keeling, C. D., Bacastow, R. B., Guenther, P. R., Lueker, T. J., Wahlen, M., Meijer, H. A. J., Mook, W. G., and Stocker, T. F.: Spatiotemporal patterns of carbon-13 in the global surface oceans and the oceanic suess effect, Global Biogeochemical Cycles, 13, 307-335, doi:10.1029/1999GB900019, 1999.

Gruber, N., and Keeling, C. D.: An improved estimate of the isotopic air-sea disequilibrium of CO2: Implications for the oceanic uptake of anthropogenic CO2, Geophysical Research Letters, 28, 555-558, 10.1029/2000GL011853, 2001.

Heinze, C., Maier-Reimer, E., and Winn, K.: Glacial pCO_2 Reduction by the World Ocean: Experiments With the Hamburg Carbon Cycle Model, Paleoceanography, 6, 395-430, 10.1029/91PA00489, 1991.

Heinze, C., and Hasselmann, K.: Inverse Multiparameter Modeling of Paleoclimate Carbon Cycle Indices, Quaternary Research, 40, 281-296, https://doi.org/10.1006/qres.1993.1082, 1993.

Heinze, C., and Maier-Reimer, E.: The Hamburg Oceanic Carbon Cycle Circulation Model Version "HAMOCC2s" for long time integrations, Max-Planck-Institut für Meteorologie, Hamburg REPORT 20, 1999.

Heinze, C.: Assessing the importance of the Southern Ocean for natural atmospheric pCO_2 variations with a global biogeochemical general circulation model, Deep Sea Research Part II: Topical Studies in Oceanography, 49, 3105-3125, http://dx.doi.org/10.1016/S0967-0645(02)00074-7, 2002.

Heinze, C., Hoogakker, B. A. A., and Winguth, A.: Ocean carbon cycling during the past 130 000 years – a pilot study on inverse palaeoclimate record modelling, Clim. Past, 12, 1949-1978, 10.5194/cp-12-1949-2016, 2016.

Hilting, A. K., Kump, L. R., and Bralower, T. J.: Variations in the oceanic vertical carbon isotope gradient and their implications for the Paleocene-Eocene biological pump, Paleoceanography, 23, n/a-n/a, 10.1029/2007PA001458, 2008.

Holden, P. B., Edwards, N. R., Müller, S. A., Oliver, K. I. C., Death, R. M., and Ridgwell, A.: Controls on the spatial distribution of oceanic δ13C_DIC, Biogeosciences, 10, 1815-1833, 10.5194/bg-10-1815-2013, 2013.

Hollander, D. J., and McKenzie, J. A.: CO2 control on carbon-isotope fractionation during aqueous photosynthesis: A paleo-pCO_2 barometer, Geology, 19, 929-932, 10.1130/0091-7613(1991)019<0929:ccocif>2.3.co;2, 1991.

Hoogakker, B. A. A., Elderfield, H., Schmiedl, G., McCave, I. N., and Rickaby, R. E. M.: Glacial-interglacial changes in bottom-water oxygen content on the Portuguese margin, Nature Geosci, 8, 40-43, 10.1038/ngeo2317 http://www.nature.com/ngeo/journal/v8/n1/abs/ngeo2317.html#supplementary-information, 2015.

Jahn, A., Lindsay, K., Giraud, X., Gruber, N., Otto-Bliesner, B. L., Liu, Z., and Brady, E. C.: Carbon isotopes in the ocean model of the Community Earth System Model (CESM1), Geoscientific Model Development, 8, 2419-2434, 10.5194/gmd-8-2419-2015, 2015.

Jansen, M. F.: Glacial ocean circulation and stratification explained by reduced atmospheric temperature, Proceedings of the National Academy of Sciences, 114, 45-50, 10.1073/pnas.1610438113, 2017.

Jones, D. C., Ito, T., Takano, Y., and Hsu, W.-C.: Spatial and seasonal variability of the air-sea equilibration timescale of carbon dioxide, Global Biogeochemical Cycles, 28, 1163-1178, 10.1002/2014GB004813, 2014.

Keir, R. S.: The effect of vertical nutrient redistribution on surface ocean δ13C, Global Biogeochemical Cycles, 5, 351-358, doi:10.1029/91GB01913, 1991.

Kroopnick, P.: The distribution of 13C in the Atlantic Ocean, Earth and Planetary Science Letters, 49, 469-484, https://doi.org/10.1016/0012-821X(80)90088-6, 1980.

Kroopnick, P. M.: The distribution of 13C of ΣCO2 in the world oceans, Deep Sea Research Part A. Oceanographic Research Papers, 32, 57-84, https://doi.org/10.1016/0198-0149(85)90017-2, 1985.
Laws, E. A., Bidigare, R., R., and Popp, B. N.: Effects of growth rate and CO2 concentration on carbon isotopic fractionation by the marine diatom Phaeodactylum tricornutum, Limnol. Oceanogr., 42, 1552-1560, 1997.
Lear, C. H., Billups, K., Rickaby, R. E. M., Diester-Haass, L., Mawbey, E. M., and Sosdian, S. M.: Breathing more deeply: Deep ocean carbon storage during the mid-Pleistocene climate transition, Geology, 44, 1035-1038, 10.1130/G38636.1, 2016.
Lisiecki, L. E.: A benthic δ13C-based proxy for atmospheric pCO2 over the last 1.5 Myr, Geophysical Research Letters, 37, 10.1029/2010GL045109, 2010.
Lourantou, A., Lavrič Jošt, V., Köhler, P., Barnola, J. M., Paillard, D., Michel, E., Raynaud, D., and Chappellaz, J.: Constraint of the CO2 rise by new atmospheric carbon isotopic measurements during the last deglaciation, Global Biogeochemical Cycles, 24, 10.1029/2009GB003545, 2010.
Lutz, M. J., Caldeira, K., Dunbar, R. B., and Behrenfeld, M. J.: Seasonal rhythms of net primary production and particulate organic carbon flux to depth describe the efficiency of biological pump in the global ocean, Journal of Geophysical Research: Oceans, 112, C10011, 10.1029/2006JC003706, 2007.
Lynch-Stieglitz, J., Stocker, T. F., Broecker, W. S., and Fairbanks, R. G.: The influence of air-sea exchange on the isotopic composition of oceanic carbon: Observations and modeling, Global Biogeochemical Cycles, 9, 653-665, 10.1029/95GB02574, 1995.
MacCready, P., and Quay, P.: Biological export flux in the Southern Ocean estimated from a climatological nitrate budget, Deep Sea Research Part II: Topical Studies in Oceanography, 48, 4299-4322, http://dx.doi.org/10.1016/S0967-0645(01)00090-X, 2001.
Mackenzie, F. T., and Lerman, A.: Isotopic Fractionation of Carbon: Inorganic and Biological Processes, in: Carbon in the Geobiosphere — Earth's Outer Shell —, edited by: Mackenzie, F. T., and Lerman, A., Springer Netherlands, Dordrecht, 165-191, 2006.
Marchal, O., Stocker, T. F., and Joos, F.: A latitude-depth, circulation-biogeochemical ocean model for paleoclimate studies. Development and sensitivities, Tellus B, 50, 290-316, 10.1034/j.1600-0889.1998.t01-2-00006.x, 1998.
Marinov, I., Gnanadesikan, A., Toggweiler, J. R., and Sarmiento, J. L.: The Southern Ocean biogeochemical divide, Nature, 441, 964-967, http://www.nature.com/nature/journal/v441/n7096/suppinfo/nature04883.html, 2006.
Menviel, L., Mouchet, A., Meissner, K. J., Joos, F., and England, M. H.: Impact of oceanic circulation changes on atmospheric δ13CO2, Global Biogeochemical Cycles, 29, 1944-1961, 10.1002/2015GB005207, 2015.
Menviel, L., Yu, J., Joos, F., Mouchet, A., Meissner, K. J., and England, M. H.: Poorly ventilated deep ocean at the Last Glacial Maximum inferred from carbon isotopes: A data-model comparison study, Paleoceanography, 32, 2-17, 10.1002/2016PA003024, 2016.
Milliman, J. D., and Droxler, A. W.: Neritic and pelagic carbonate sedimentation in the marine environment: ignorance is not bliss, Geologische Rundschau, 85, 496-504, 10.1007/BF02369004, 1996.
Mook, W. G.: 13C in atmospheric CO2, Netherlands Journal of Sea Research, 20, 211-223, http://dx.doi.org/10.1016/0077-7579(86)90043-8, 1986.
Mulitza, S., Rühlemann, C., Bickert, T., Hale, W., Pätzold, J., and Wefer, G.: Late Quaternary δ13C gradients and carbonate accumulation in the western equatorial Atlantic, Earth and Planetary Science Letters, 155, 237-249, https://doi.org/10.1016/S0012-821X(98)00012-0, 1998.
Murnane, R. J., and Sarmiento, J. L.: Roles of biology and gas exchange in determining the δ13C distribution in the ocean and the preindustrial gradient in atmospheric δ13C, Global Biogeochemical Cycles, 14, 389-405, 10.1029/1998GB001071, 2000.
Nevison, C. D., Keeling, R. F., Kahru, M., Manizza, M., Mitchell, B. G., and Cassar, N.: Estimating net community production in the Southern Ocean based on atmospheric potential oxygen and satellite ocean color data, Global Biogeochemical Cycles, 26, GB1020, 10.1029/2011GB004040, 2012.
Oliver, K. I. C., Hoogakker, B. A. A., Crowhurst, S., Henderson, G. M., Rickaby, R. E. M., Edwards, N. R., and Elderfield, H.: A synthesis of marine sediment core δ13C data over the last 150 000 years, Climate of the Past, 6, 645-673, 2010.
Oppo, D. W., Fairbanks, R. G., and Gordon, A. L.: Late Pleistocene Southern Ocean δ13C variability, Paleoceanography, 5, 43-54, 10.1029/PA005i001p00043, 1990.
Primeau, F. W., Holzer, M., and DeVries, T.: Southern Ocean nutrient trapping and the efficiency of the biological pump, Journal of Geophysical Research: Oceans, 118, 2547-2564, 10.1002/jgrc.20181, 2013.

Quay, P., Sonnerup, R., Westby, T., Stutsman, J., and McNichol, A.: Changes in the 13C/12C of dissolved inorganic carbon in the ocean as a tracer of anthropogenic CO2 uptake, Global Biogeochemical Cycles, 17, 4-1-4-20, 10.1029/2001GB001817, 2003.

Roth, R., Ritz, S. P., and Joos, F.: Burial-nutrient feedbacks amplify the sensitivity of atmospheric carbon dioxide to changes in organic matter remineralisation, Earth Syst Dynam, 5, 321-343, 10.5194/esd-5-321-2014, 2014.

Sarmiento, J. L., Gruber, N., Brzezinski, M. A., and Dunne, J. P.: High-latitude controls of thermocline nutrients and low latitude biological productivity, Nature, 427, 56-60, 2004.

Schlitzer, R.: Carbon Export Fluxes in the Southern Ocean: Results from Inverse Modeling and Comparison with Satellite Estimates, Deep Sea Research, 2, 1623-1644, 2002.

Schmittner, A., Gruber, N., Mix, A. C., Key, R. M., Tagliabue, A., and Westberry, T. K.: Biology and air-sea gas exchange controls on the distribution of carbon isotope ratios (δ13C) in the ocean, Biogeosciences, 10, 5793-5816, 10.5194/bg-10-5793-2013, 2013.

Schmittner, A., and Somes, C. J.: Complementary constraints from carbon (13C) and nitrogen (15N) isotopes on the glacial ocean's soft-tissue biological pump, Paleoceanography, 31, 669-693, 10.1002/2015PA002905, 2016.

Shackleton, N. J., Hall, M. A., Line, J., and Shuxi, C.: Carbon isotope data in core V19-30 confirm reduced carbon dioxide concentration in the ice age atmosphere, Nature, 306, 319, 10.1038/306319a0, 1983.

Shackleton, N. J., and Pisias, N. G.: Atmospheric carbon dioxide, orbital forcing, and climate, in: The Carbon cycle and atmospheric CO2: natural variations archean to present, edited by: Sundquist, E. T., and Broecker, W. S., Geophysical Monograph, American Geophysical Union, Washington, 303-317, 1985.

Sonnerup, R. E., and Quay, P. D.: 13C constraints on ocean carbon cycle models, Global Biogeochemical Cycles, 26, GB2014, 10.1029/2010GB003980, 2012.

Stephens, B. B., and Keeling, R. F.: The influence of Antarctic sea ice on glacial–interglacial CO2 variations, Nature, 404, 171, 10.1038/35004556, 2000.

Tagliabue, A., and Bopp, L.: Towards understanding global variability in ocean carbon-13, Global Biogeochemical Cycles, 22, GB1025, 10.1029/2007GB003037, 2008.

Toggweiler, J. R.: Variation of atmospheric CO2 by ventilation of the ocean's deepest water, Paleoceanography, 14, 571-588, 10.1029/1999PA900033, 1999.

Tréguer, P.: Silica and the cycle of carbon in the ocean, Comptes Rendus Geoscience, 334, 3-11, https://doi.org/10.1016/S1631-0713(02)01680-2, 2002.

Tschumi, T., Joos, F., Gehlen, M., and Heinze, C.: Deep ocean ventilation, carbon isotopes, marine sedimentation and the deglacial CO2 rise, Clim. Past, 7, 771-800, https://doi.org/10.5194/cp-7-771-2011, 2011.

Zahn, R., Winn, K., and Sarnthein, M.: Benthic foraminiferal δ13C and accumulation rates of organic carbon: Uvigerina Peregrina group and Cibicidoides Wuellerstorfi, Paleoceanography, 1, 27-42, 10.1029/PA001i001p00027, 1986.

Zeebe, R., and Wolf-Gladrow, D.: CO2 in Seawater: Equilibrium, Kinetics, Isotopes, Elsevier Oceanography Series, edited by: Halpern, D., Elsevier Science B.V., Amsterdam, The Netherlands, 346 pp., 2001.

Zhang, J., Quay, P. D., and Wilbur, D. O.: Carbon isotope fractionation during gas-water exchange and dissolution of CO2, Geochimica et Cosmochimica Acta, 59, 107-114, http://dx.doi.org/10.1016/0016-7037(95)91550-D, 1995.

Ziegler, M., Diz, P., Hall, I. R., and Zahn, R.: Millennial-scale changes in atmospheric CO2 levels linked to the Southern Ocean carbon isotope gradient and dust flux, Nature Geosci, 6, 457-461, 10.1038/ngeo1782 http://www.nature.com/ngeo/journal/v6/n6/abs/ngeo1782.html#supplementary-information, 2013.

Experiment	Experiment setup
Gas fast	CO_2 gas exchange rate * 4
Gas slow	CO_2 gas exchange rate / 4
Efficient biological pump	POC sinking rate doubled to 6m/d
Inefficient biological pump	POC sinking rate halved to 1.5m/d
V_{max}	High nutrient uptake rate (control*5) in the Southern Ocean
Ice large	Southern Ocean sea ice cover south of 50° S
Ice small	Southern Ocean sea ice cover south of 70° S

Table 1 Description of the sensitivity experiments. The sensitivity experiments on the CO_2 gas exchange rate and the biological pump have been done twice, once for the Global Ocean and once only making changes in the Southern Ocean (south of 45° S).

	Global experiments		SO-only experiments	
	pCO_2^{atm}	$\delta^{13}C^{atm}$	pCO_2^{atm}	$\delta^{13}C^{atm}$
Control	279	-6,54	-	
Gas exchange				
Fast	27588	-6,8	27884	-7,06,9
Slow	2894	-6,3	2831	-6,21
Biological pump				
POC: Efficient	2562	-6,32	275	-6,54
POC: Inefficient	2923	-6,7	2823	-6,5
V_{max}	-		23529	-6,10
Ice				
Large	-		2874	-6,21
Small	-		2724	-6,6

Table 2 Results of pCO_2^{atm} [ppm] and $\delta^{13}C^{atm}$ [‰] for all sensitivity experiments.

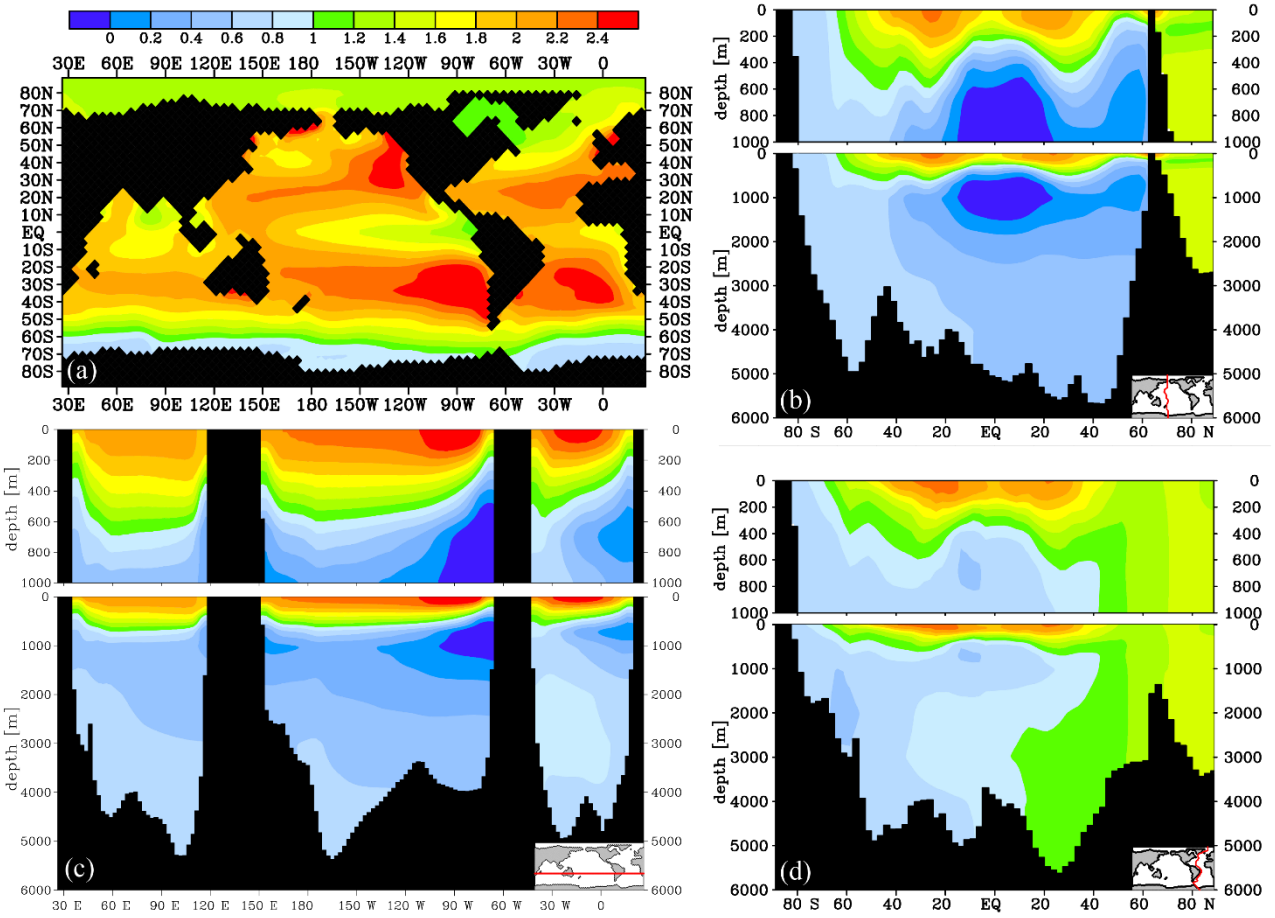

Figure 1 Modelled $\delta^{13}C$ of DIC [‰] distribution for the model control run: (a) $\delta^{13}C$ at 25 m depth, (b) Pacific transect of $\delta^{13}C$, (c) ~~Z~~zonal transect of $\delta^{13}C$ at 26° S, and (d) Atlantic transect of $\delta^{13}C$.

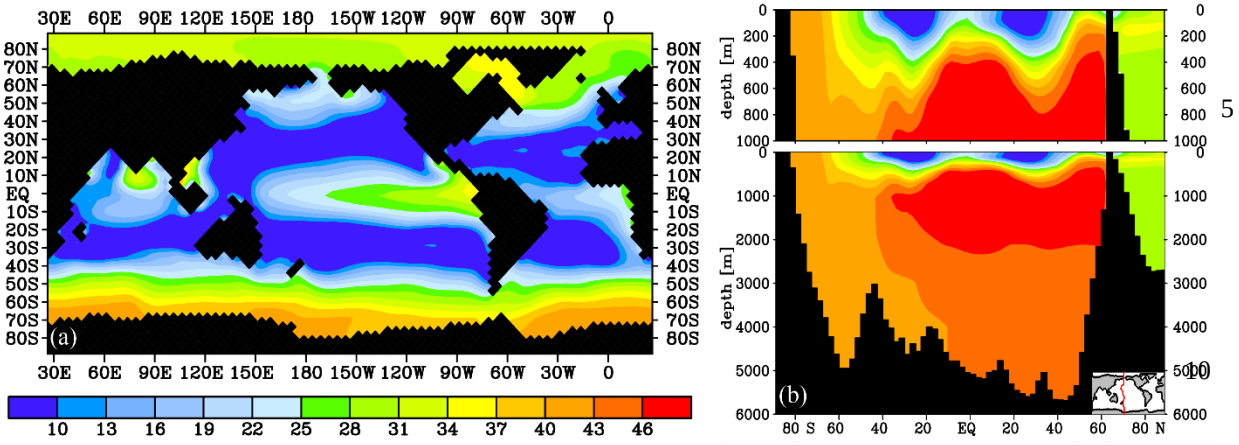

Figure 2 $\delta^{13}C_{bio}^{perc}$, the contribution of biology to the local $\delta^{13}C$ signal [%], as calculated using Eq. (4) at (a) 25 m depth and (b) a Pacific transect. The remainder of 100 % is attributed to air-sea gas exchange. The $\delta^{13}C_{bio}$ and $\delta^{13}C_{AS}$ values in ‰ are very similar to the values found by Schmittner et al. (2013).

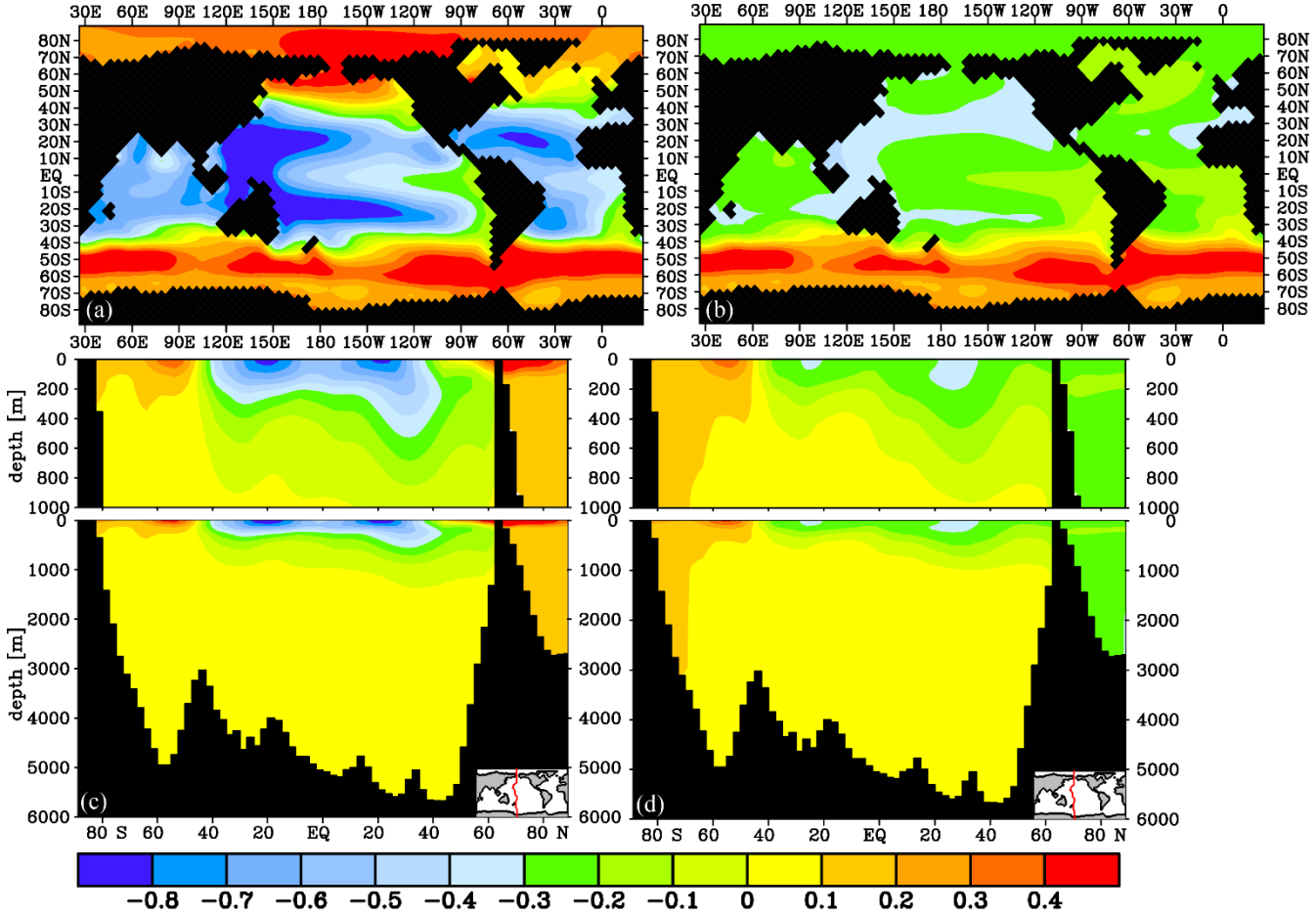

Figure 3 δ^{13}C of DIC [‰] difference after 2000 years for the fast gas exchange experiments (~~M~~experiment~~odelled~~ – control)~~fast gas exchange sensitivity experiment δ^{13}C of DIC [‰] difference with the model control run~~: global experiments (a) and (c) and SO-only experiments (b) and (d), at 25 m depth (a) and (b) and as a Pacific transect of δ^{13}C difference (c) and (d).

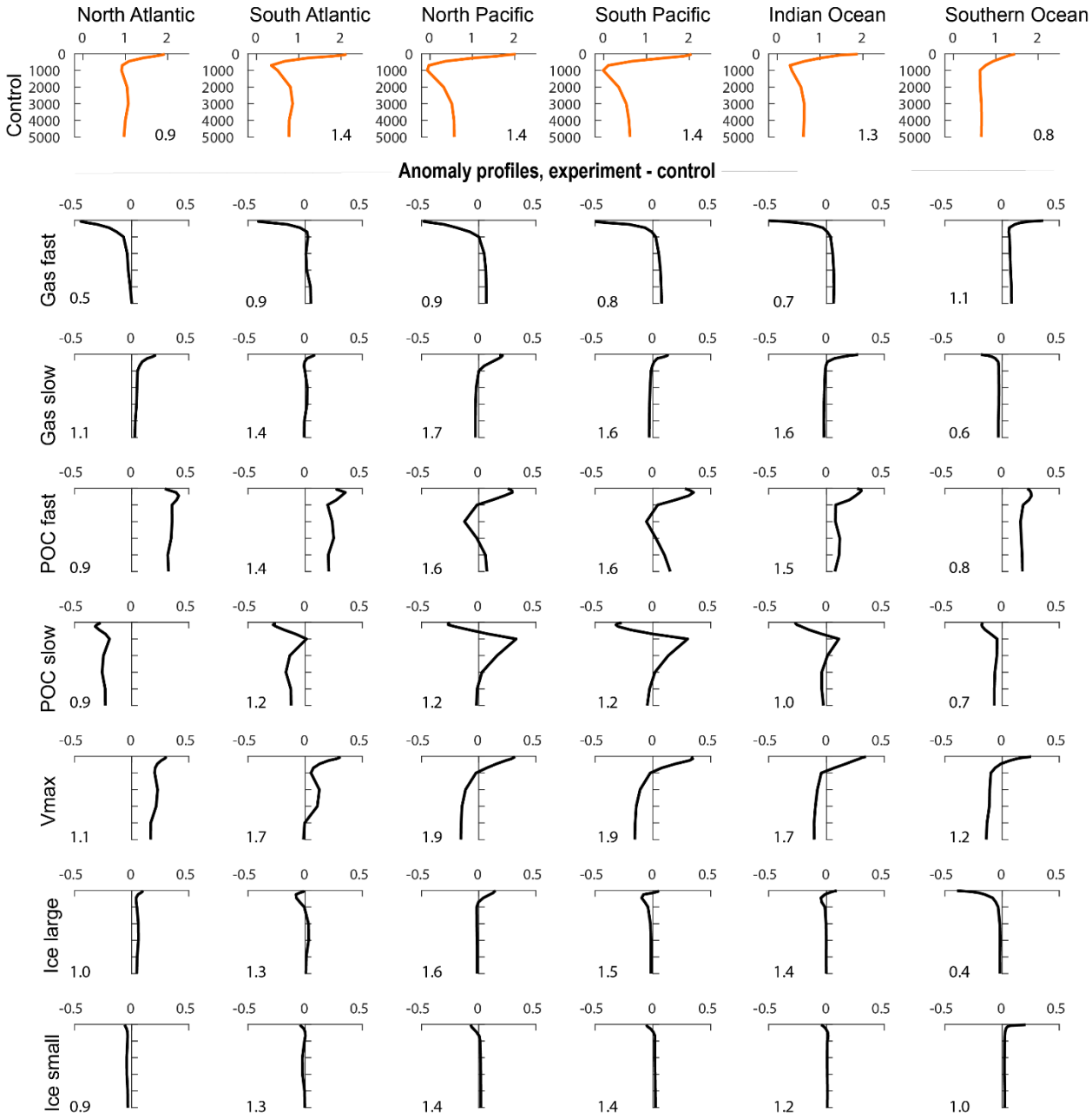

Figure 4 Volume-weighted basin mean anomaly profiles of $\delta^{13}C$ after 2000 years, with respect to the control profiles (upper row). ~~, with~~ $\Delta\delta^{13}C$ denoted per basin in the lower right (control) and lower left (sensitivity experiments) corner of each subgraph~~profile for the sensitivity experiments (thick black lines~~. Results are presented for the g~~, G~~lobal ~~for~~ gas exchange and POC sinking experiments~~)~~. Basin extent is visualised in Fig. S8~~11~~. ~~The thin orange line represents the control model run, which has a $\Delta\delta^{13}C$ of 0.9 (North Atlantic), 1.3 (South Atlantic), 1.4 (North Pacific), 1.4 (South Pacific), 1.2 (Indian Ocean) and 0.8 (Southern Ocean). See Fig. S7 for the resulting anomaly profiles for each experiment.~~

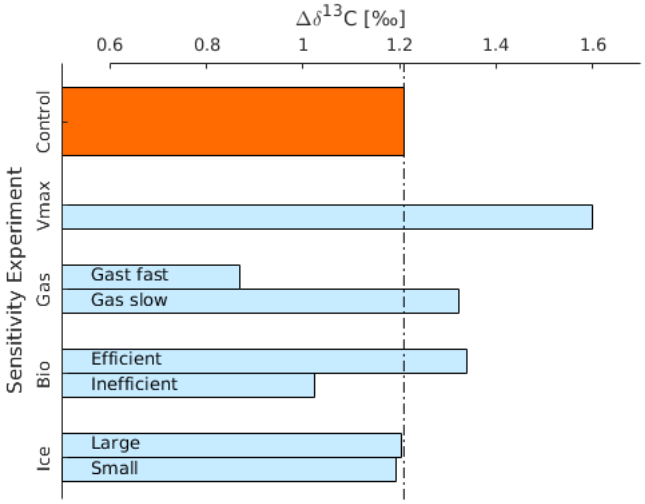

Figure 5 Global mean $\Delta\delta^{13}C$ after 2000 years for the different sensitivity experiments (Table 1). 'Bio Efficient' represents the high POC sinking rate experiment, 'Bio Inefficient' the slow POC sinking rate experiment. The results for the Southern Ocean-only experiments (Sect. 2) are described in the text.

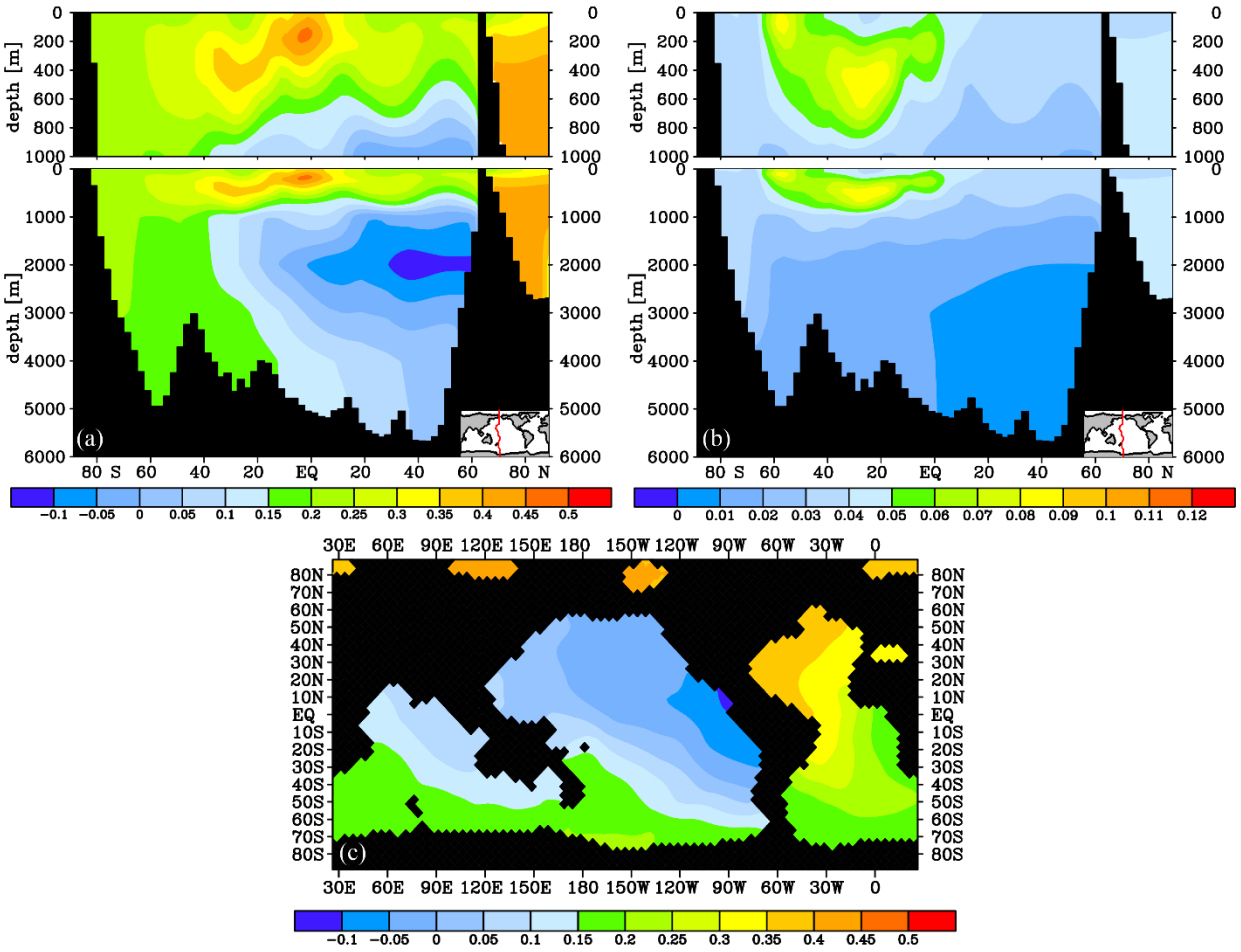

Figure 6 δ^{13}C of DIC [‰] difference after 2000 years for the POC sinking rate experiments (experiment – control): ~~δ^{13}C of DIC difference between model control run and~~ **(a) the global efficient biological pump (high POC sinking rate) experiment for a Pacific transect and (b) the SO-only efficient biological pump** ~~(high POC sinking rate)~~ **experiment for a Pacific transect and (c)** the global efficient biological pump experiment **at 3000m depth** ~~for the global efficient biological pump experiment~~**. Note the different scales.**

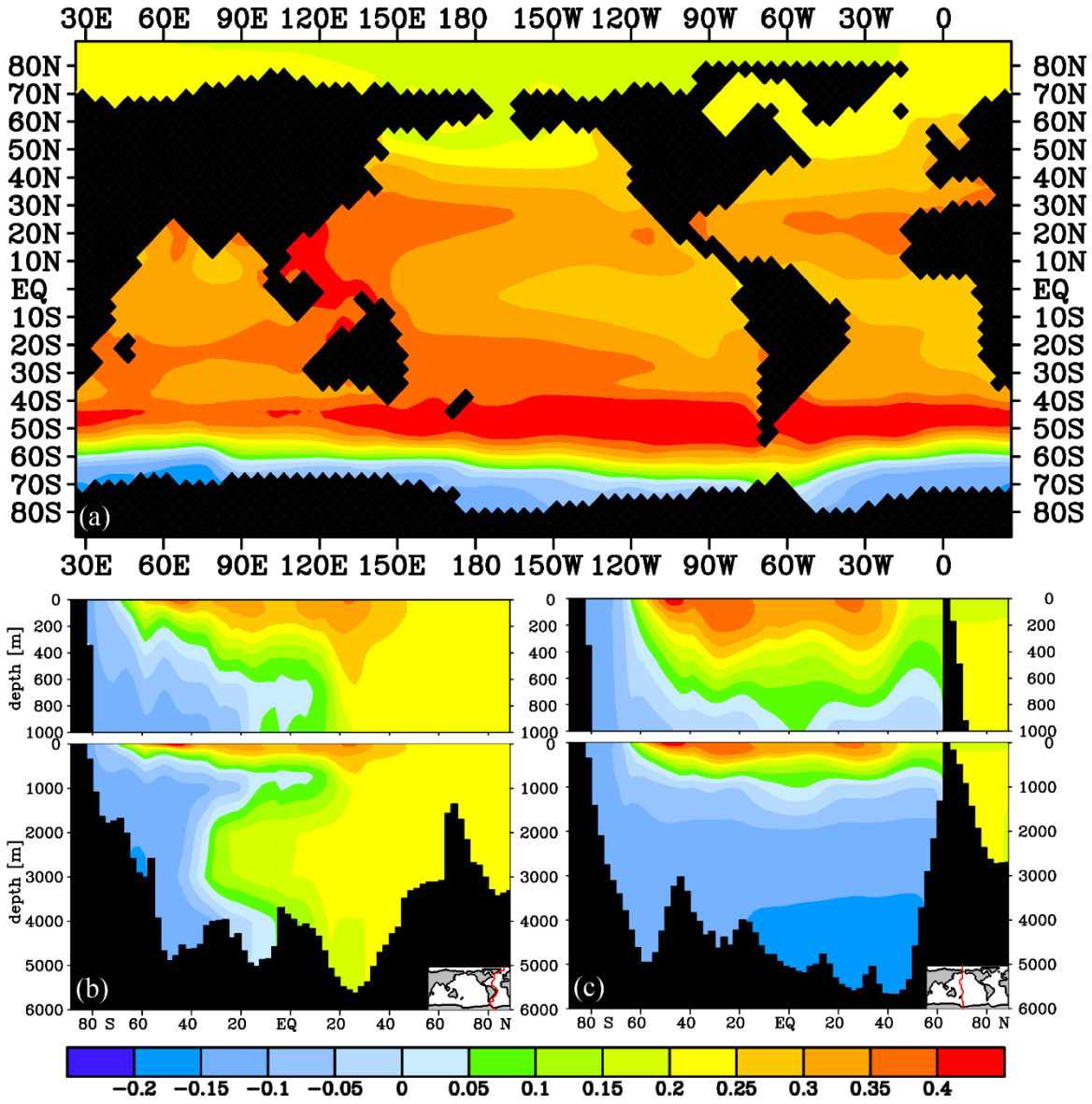

Figure 7 ~~Dδ13C of DIC [‰] difference after 2000 years for the Vmax nutrient depletion experiment (experiment – control): ifference plots between the model control run and the Vmax nutrient depletion experiment at~~ **(a)** at **25m depth and for (b) an Atlantic transect and (c) a Pacific transect.**

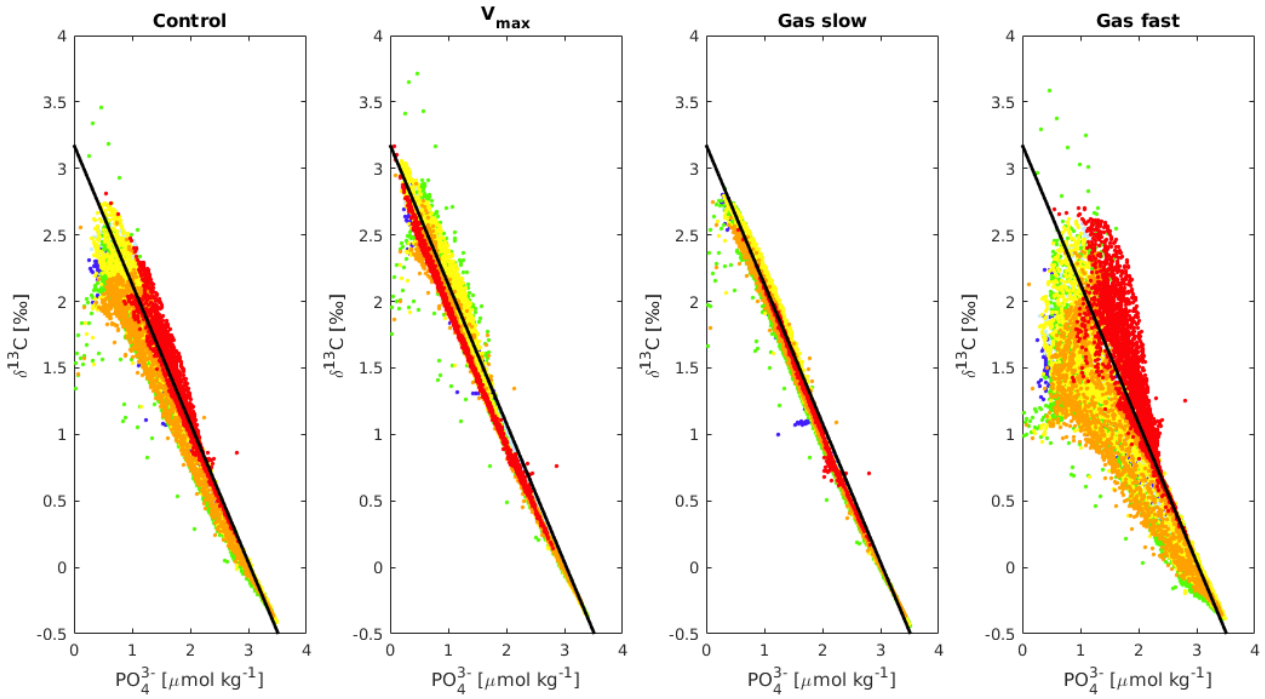

Figure 8 $\delta^{13}C$ versus PO_4^{3-} for the control, V_{max}, 'Gas slow' and 'Gas fast' experiments for all ocean basins except the Nordic Seas (i.e. basins A to F in Fig. S8). Dark blue = A / North Atlantic, Light blue = B / South Atlantic, Red = C / Southern Ocean, Yellow = D / South Pacific, Green = E / North Pacific, Orange = F / Indian Ocean. The black line is the $\delta^{13}C_{bio}$=3.18-1.05* PO_4^{3-} relationship, i.e. the relationship between $\delta^{13}C$ and PO_4^{3-} expected if only biology affected $\delta^{13}C$ (Sect. 2). Deviations from the black line represent the relative importance of air-sea gas exchange as compared to biology for $\delta^{13}C$.

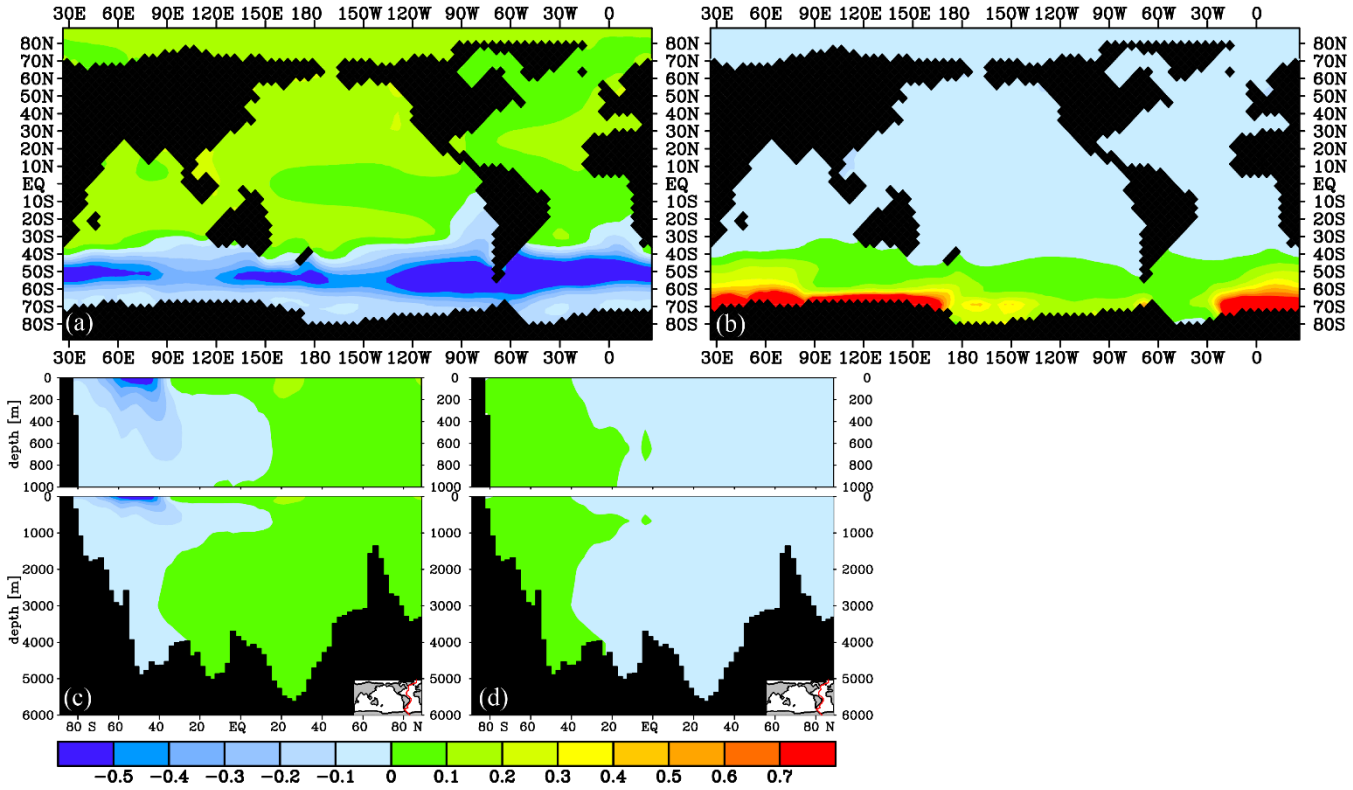

Figure ~~98~~ δ13C of DIC [‰] difference after 2000 years for the Antarctic sea ice cover experiments (experiment – control): The effect of a large (a, c) and small (b, d) Antarctic sea ice cover~~, on $\delta^{13}C$ as compared to the control~~ for 25 m depth (a, b) and an

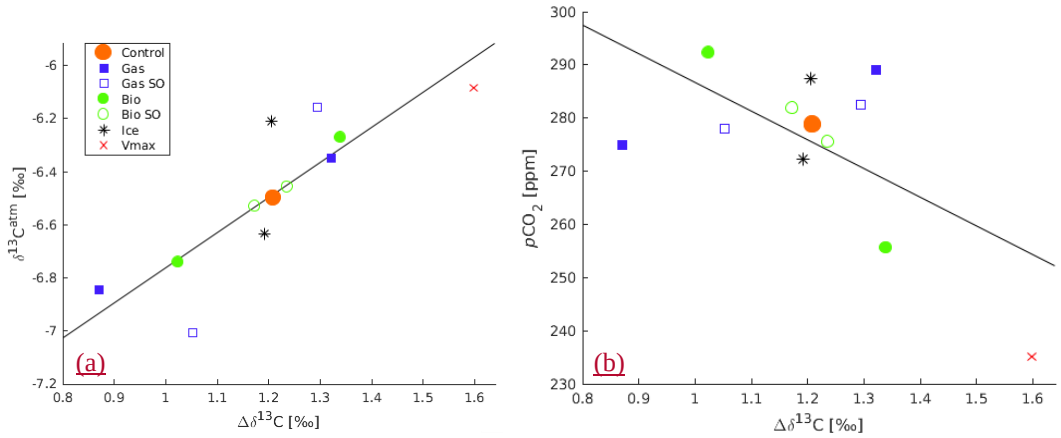

Figure 10~~9~~ Relationships between global mean $\Delta\delta^{13}C$, $\delta^{13}C^{atm}$ and pCO_2^{atm}. ~~Scatter plot of the global mean $\Delta\delta^{13}C$, $\delta^{13}C$ and~~ (a) Global mean $\Delta\delta^{13}C$ versus $\delta^{13}C^{atm}$ of the different sensitivity experiments. R^2 ~~squared~~ of the best-fit line is 0.73 (p-0.713 ~~(p-value 0.0004)~~, and the line is described by y=1.3x-~~8~~7.1~~95~~ (b) Global mean $\Delta\delta^{13}C$ versus pCO_2^{atm} of the different different sensitivity experiments. R^2 ~~squared~~ of the best-fit line is 0.39~~655 (p-value 0.00143)~~, and the line is described by y=-by y=-~~5475~~x+34~~165~~.